3D angular momentum and particle number restored calculations with the Gogny EDF

Tomás R. Rodríguez

GSI theory

HIC for FAIR
Helmholtz International Center

Outline

1. Theoretical framework
2. Applications
3. Conclusions and outlook

Solving the nuclear many body problem

In order to give a proper description of the nuclear system we need:

➡ A good **interaction** or energy density functional (EDF) that describes the dynamics of the constituent nucleons.

➡ A good **method** -adapted to the corresponding interaction/EDF- for solving the quantum many body problem.

CONTENTS

Solving the nuclear many body problem

In order to give a proper description of the nuclear system we need:

➡ A good **interaction** or energy density functional (EDF) that describes the dynamics of the constituent nucleons.

➡ A good **method** -adapted to the corresponding interaction/EDF- for solving the quantum many body problem.

Some considerations:

- Both mean field (SR-EDF) and beyond mean field (MR-EDF) methods use intrinsic many-body auxiliary wave functions.

Solving the nuclear many body problem

In order to give a proper description of the nuclear system we need:

➡ A good **interaction** or energy density functional (EDF) that describes the dynamics of the constituent nucleons.

➡ A good **method** -adapted to the corresponding interaction/EDF- for solving the quantum many body problem.

Some considerations:

- Both mean field (SR-EDF) and beyond mean field (MR-EDF) methods use intrinsic many-body auxiliary wave functions.
- Density matrices (normal and abnormal) and spatial densities are written in terms of these auxiliary wave functions.

Solving the nuclear many body problem

CONTENTS

In order to give a proper description of the nuclear system we need:

➡ A good **interaction** or energy density functional (EDF) that describes the dynamics of the constituent nucleons.

➡ A good **method** -adapted to the corresponding interaction/EDF- for solving the quantum many body problem.

Some considerations:

- Both mean field (SR-EDF) and beyond mean field (MR-EDF) methods use intrinsic many-body auxiliary wave functions.
- Density matrices (normal and abnormal) and spatial densities are written in terms of these auxiliary wave functions.
- All the observables and variational procedures in EDF methods are expressed in terms of density matrices and spatial densities.

Solving the nuclear many body problem

CONTENTS

In order to give a proper description of the nuclear system we need:

➡ A good **interaction** or energy density functional (EDF) that describes the dynamics of the constituent nucleons.

➡ A good **method** -adapted to the corresponding interaction/EDF- for solving the quantum many body problem.

Some considerations:

- Both mean field (SR-EDF) and beyond mean field (MR-EDF) methods use intrinsic many-body auxiliary wave functions.
- Density matrices (normal and abnormal) and spatial densities are written in terms of these auxiliary wave functions.
- All the observables and variational procedures in EDF methods are expressed in terms of density matrices and spatial densities.
- The usual EDF methods consist in determining first the "best" auxiliary many body wave functions and, afterwards, in including more correlations.

CONTENTS

Theoretical Framework

- Initial intrinsic states: PN-VAP $\delta E^{N,Z}\left[\bar{\Phi}(\beta,\gamma)\right]\Big|_{\bar{\Phi}=\Phi}=0$

$$E^{N,Z}[\Phi]=\frac{\langle\Phi|\hat{H}_{2b}\hat{P}^{N}\hat{P}^{Z}|\Phi\rangle}{\langle\Phi|\hat{P}^{N}\hat{P}^{Z}|\Phi\rangle}+\varepsilon_{DD}^{N,Z}(\Phi)-\lambda_{q_{20}}\langle\Phi|\hat{Q}_{20}|\Phi\rangle-\lambda_{q_{22}}\langle\Phi|\hat{Q}_{22}|\Phi\rangle$$

- Intermediate Particle Number and Angular Momentum Projected states

$$|IMK;NZ;\beta\gamma\rangle=\frac{2I+1}{8\pi^{2}}\int\mathcal{D}^{I*}_{MK}(\Omega)\hat{R}(\Omega)\hat{P}^{N}\hat{P}^{Z}|\Phi(\beta,\gamma)\rangle d\Omega$$

- Final GCM states $|IM;NZ\sigma\rangle=\sum_{K\beta\gamma}f^{I;NZ,\sigma}_{K\beta\gamma}|IMK;NZ;\beta\gamma\rangle$

$$\sum_{K'\beta'\gamma'}\left(\mathcal{H}^{I;NZ}_{K\beta\gamma K'\beta'\gamma'}-E^{I;NZ;\sigma}\mathcal{N}^{I;NZ}_{K\beta\gamma K'\beta'\gamma'}\right)f^{I;NZ;\sigma}_{K'\beta'\gamma'}=0$$

$$\mathcal{N}^{I;NZ}_{K\beta\gamma K'\beta'\gamma'}\equiv\langle IMK;NZ;\beta\gamma|IMK';NZ;\beta'\gamma'\rangle$$
$$\mathcal{H}^{I;NZ}_{K\beta\gamma K'\beta'\gamma'}\equiv\langle IMK;NZ;\beta\gamma|\hat{H}_{2b}|IMK';NZ;\beta'\gamma'\rangle+\varepsilon_{DD}^{IKK';NZ}\left[\Phi(\beta,\gamma),\Phi'(\beta',\gamma')\right]$$

CONTENTS

1. Theoretical framework

2. Applications

3. Conclusions and outlook

Theoretical Framework

- Initial intrinsic states: PN-VAP $\delta E^{N,Z}\left[\bar{\Phi}(\beta,\gamma)\right]\Big|_{\bar{\Phi}=\Phi}=0$

$$E^{N,Z}[\Phi]=\frac{\langle\Phi|\hat{H}_{2\mathrm{b}}\hat{P}^{N}\hat{P}^{Z}|\Phi\rangle}{\cdots}+\varepsilon_{DD}^{N,Z}(\Phi)-\lambda_{q_{20}}\langle\Phi|\hat{Q}_{20}|\Phi\rangle-\lambda_{q_{22}}\langle\Phi|\hat{Q}_{22}|\Phi\rangle$$

Recent 3D AMP implementations

Skyrme: M. Bender, P.-H. Heenen, Phys. Rev. C 78, 024309 (2008)
- Particle number and angular momentum restoration of intrinsic LN states.

Relativistic: J.M. Yao et al., Phys. Rev. C 81, 04431 (2010)
- Angular momentum restoration of intrinsic HFB states.

Gogny: T.R.R., J.L. Egido, Phys. Rev C 81, 064323 (2010)
- Particle number and angular momentum restoration of PN-VAP states.

- Int…

states…

- Fin…

$$\sum_{K'\beta'\gamma'}\left(\mathcal{H}^{I;NZ}_{K\beta\gamma K'\beta'\gamma'}-E^{I;NZ;\sigma}\mathcal{N}^{I;NZ}_{K\beta\gamma K'\beta'\gamma'}\right)f^{I;NZ;\sigma}_{K'\beta'\gamma'}=0$$

$$\mathcal{N}^{I;NZ}_{K\beta\gamma K'\beta'\gamma'}\equiv\langle IMK;NZ;\beta\gamma|IMK';NZ;\beta'\gamma'\rangle$$

$$\mathcal{H}^{I;NZ}_{K\beta\gamma K'\beta'\gamma'}\equiv\langle IMK;NZ;\beta\gamma|\hat{H}_{2\mathrm{b}}|IMK';NZ;\beta'\gamma'\rangle+\varepsilon_{DD}^{IKK';NZ}\left[\Phi(\beta,\gamma),\Phi'(\beta',\gamma')\right]$$

CONTENTS

Theoretical Framework

- Initial intrinsic states: PN-VAP $\delta E^{N,Z}\left[\bar{\Phi}(\beta,\gamma)\right]\Big|_{\bar{\Phi}=\Phi}=0$

$$E^{N,Z}[\Phi]=\frac{\langle\Phi|\hat{H}_{2b}\hat{P}^N\hat{P}^Z|\Phi\rangle}{\langle\Phi|\hat{P}^N\hat{P}^Z|\Phi\rangle}+\varepsilon_{DD}^{N,Z}(\Phi)-\lambda_{q_{20}}\langle\Phi|\hat{Q}_{20}|\Phi\rangle-\lambda_{q_{22}}\langle\Phi|\hat{Q}_{22}|\Phi\rangle$$

- Intermediate Particle Number and Angular Momentum Projected states

$$|IMK;NZ;\beta\gamma\rangle=\frac{2I+1}{8\pi^2}\int\mathcal{D}_{MK}^{I*}(\Omega)\hat{R}(\Omega)\hat{P}^N\hat{P}^Z|\Phi(\beta,\gamma)\rangle d\Omega$$

- Final GCM states $|IM;NZ\sigma\rangle=\sum_{K\beta\gamma}f_{K\beta\gamma}^{I;NZ,\sigma}|IMK;NZ;\beta\gamma\rangle$

$$\sum_{K'\beta'\gamma'}\left(\mathcal{H}_{K\beta\gamma K'\beta'\gamma'}^{I;NZ}-E^{I;NZ;\sigma}\mathcal{N}_{K\beta\gamma K'\beta'\gamma'}^{I;NZ}\right)f_{K'\beta'\gamma'}^{I;NZ;\sigma}=0$$

$$\begin{aligned}\mathcal{N}_{K\beta\gamma K'\beta'\gamma'}^{I;NZ}&\equiv\langle IMK;NZ;\beta\gamma|IMK';NZ;\beta'\gamma'\rangle\\ \mathcal{H}_{K\beta\gamma K'\beta'\gamma'}^{I;NZ}&\equiv\langle IMK;NZ;\beta\gamma|\hat{H}_{2b}|IMK';NZ;\beta'\gamma'\rangle+\varepsilon_{DD}^{IKK';NZ}\left[\Phi(\beta,\gamma),\Phi'(\beta',\gamma')\right]\end{aligned}$$

Theoretical Framework

CONTENTS

- Initial intrinsic states: PN-VAP $\delta E^{N,Z}\left[\bar{\Phi}(\beta,\gamma)\right]\Big|_{\bar{\Phi}=\Phi}=0$

$$E^{N,Z}[\Phi]=\frac{\langle\Phi|\hat{H}_{2b}\cancel{\hat{P}^{N}\hat{P}^{Z}}|\Phi\rangle}{\langle\Phi|\cancel{\hat{P}^{N}\hat{P}^{Z}}|\Phi\rangle}+\varepsilon_{DD}^{N,Z}(\Phi)-\lambda_{q_{20}}\langle\Phi|\hat{Q}_{20}|\Phi\rangle-\lambda_{q_{22}}\langle\Phi|\hat{Q}_{22}|\Phi\rangle$$

- Intermediate Particle Number and Angular Momentum Projected states

$$|IMK;NZ;\beta\gamma\rangle=\frac{2I+1}{8\pi^{2}}\int\mathcal{D}^{I*}_{MK}(\Omega)\hat{R}(\Omega)\hat{P}^{N}\hat{P}^{Z}|\Phi(\beta,\gamma)\rangle d\Omega$$

- Final GCM states $|IM;NZ\sigma\rangle=\sum_{K\beta\gamma}f^{I;NZ,\sigma}_{K\beta\gamma}|IMK;NZ;\beta\gamma\rangle$

$$\sum_{K'\beta'\gamma'}\left(\mathcal{H}^{I;NZ}_{K\beta\gamma K'\beta'\gamma'}-E^{I;NZ;\sigma}\mathcal{N}^{I;NZ}_{K\beta\gamma K'\beta'\gamma'}\right)f^{I;NZ;\sigma}_{K'\beta'\gamma'}=0$$

$$\begin{aligned}\mathcal{N}^{I;NZ}_{K\beta\gamma K'\beta'\gamma'}&\equiv\langle IMK;NZ;\beta\gamma|IMK';NZ;\beta'\gamma'\rangle\\ \mathcal{H}^{I;NZ}_{K\beta\gamma K'\beta'\gamma'}&\equiv\langle IMK;NZ;\beta\gamma|\hat{H}_{2b}|IMK';NZ;\beta'\gamma'\rangle+\varepsilon_{DD}^{IKK';NZ}\left[\Phi(\beta,\gamma),\Phi'(\beta',\gamma')\right]\end{aligned}$$

CONTENTS

Theoretical Framework

- Initial intrinsic states: PN-VAP $\delta E^{N,Z}\left[\bar{\Phi}(\beta,\gamma)\right]\Big|_{\bar{\Phi}=\Phi}=0$

$$E^{N,Z}[\Phi]=\frac{\langle\Phi|\hat{H}_{2b}\cancel{\hat{P}^N\hat{P}^Z}|\Phi\rangle}{\langle\Phi|\cancel{\hat{P}^N\hat{P}^Z}|\Phi\rangle}+\varepsilon_{DD}^{N,Z}(\Phi)-\lambda_{q_{20}}\langle\Phi|\hat{Q}_{20}|\Phi\rangle-\lambda_{q_{22}}\langle\Phi|\hat{Q}_{22}|\Phi\rangle$$

- Intermediate Particle Number and Angular Momentum Projected states

$$|IMK;NZ;\beta\gamma\rangle=\frac{2I+1}{8\pi^2}\int\mathcal{D}^{I*}_{MK}(\Omega)\hat{R}(\Omega)\cancel{\hat{P}^N\hat{P}^Z}|\Phi(\beta,\gamma)\rangle d\Omega$$

- Final GCM states $|IM;NZ\sigma\rangle=\sum_{K\beta\gamma}f^{I;NZ,\sigma}_{K\beta\gamma}|IMK;NZ;\beta\gamma\rangle$

$$\sum_{K'\beta'\gamma'}\left(\mathcal{H}^{I;NZ}_{K\beta\gamma K'\beta'\gamma'}-E^{I;NZ;\sigma}\mathcal{N}^{I;NZ}_{K\beta\gamma K'\beta'\gamma'}\right)f^{I;NZ;\sigma}_{K'\beta'\gamma'}=0$$

$$\begin{aligned}\mathcal{N}^{I;NZ}_{K\beta\gamma K'\beta'\gamma'}&\equiv\langle IMK;NZ;\beta\gamma|IMK';NZ;\beta'\gamma'\rangle\\ \mathcal{H}^{I;NZ}_{K\beta\gamma K'\beta'\gamma'}&\equiv\langle IMK;NZ;\beta\gamma|\hat{H}_{2b}|IMK';NZ;\beta'\gamma'\rangle+\varepsilon_{DD}^{IKK';NZ}\left[\Phi(\beta,\gamma),\Phi'(\beta',\gamma')\right]\end{aligned}$$

Theoretical Framework

- Initial intrinsic states: PN-VAP $\delta E^{N,Z}\left[\bar{\Phi}(\beta,\gamma)\right]\Big|_{\bar{\Phi}=\Phi}=0$

$$E^{N,Z}[\Phi]=\frac{\langle\Phi|\hat{H}_{2b}\hat{P}^N\hat{P}^Z|\Phi\rangle}{\langle\Phi|\hat{P}^N\hat{P}^Z|\Phi\rangle}+\varepsilon_{DD}^{N,Z}(\Phi)-\lambda_{q_{20}}\langle\Phi|\hat{Q}_{20}|\Phi\rangle-\lambda_{q_{22}}\langle\Phi|\hat{Q}_{22}|\Phi\rangle$$

- Intermediate Particle Number and Angular Momentum Projected states

$$|IMK;NZ;\beta\gamma\rangle=\frac{2I+1}{8\pi^2}\int\mathcal{D}^{I*}_{MK}(\Omega)\hat{R}(\Omega)\hat{P}^N\hat{P}^Z|\Phi(\beta,\gamma)\rangle d\Omega$$

- Final GCM states $|IM;NZ\sigma\rangle=\sum_{K\beta\gamma}f^{I;NZ,\sigma}_{K\beta\gamma}|IMK;NZ;\beta\gamma\rangle$

$$\sum_{K'\beta'\gamma'}\left(\mathcal{H}^{I;NZ}_{K\beta\gamma K'\beta'\gamma'}-E^{I;NZ;\sigma}\mathcal{N}^{I;NZ}_{K\beta\gamma K'\beta'\gamma'}\right)f^{I;NZ;\sigma}_{K'\beta'\gamma'}=0$$

$$\begin{aligned}\mathcal{N}^{I;NZ}_{K\beta\gamma K'\beta'\gamma'}&\equiv\langle IMK;NZ;\beta\gamma|IMK';NZ;\beta'\gamma'\rangle\\ \mathcal{H}^{I;NZ}_{K\beta\gamma K'\beta'\gamma'}&\equiv\langle IMK;NZ;\beta\gamma|\hat{H}_{2b}|IMK';NZ;\beta'\gamma'\rangle+\varepsilon_{DD}^{IKK';NZ}\left[\Phi(\beta,\gamma),\Phi'(\beta',\gamma')\right]\end{aligned}$$

Theoretical Framework

Effective nucleon-nucleon interaction:
Gogny force (D1S) that is able to describe properly many phenomena along the whole nuclear chart.

$$V(1,2) = \sum_{i=1}^{2} e^{-(\vec{r}_1-\vec{r}_2)^2/\mu_i^2} \left(W_i + B_i P^\sigma - H_i P^\tau - M_i P^\sigma P^\tau\right)$$

$$+iW_0(\sigma_1+\sigma_2)\vec{k}\times\delta(\vec{r}_1-\vec{r}_2)\vec{k} + V_{\text{Coulomb}}(\vec{r}_1,\vec{r}_2)$$

$$+t_3(1+x_0P^\sigma)\delta(\vec{r}_1-\vec{r}_2)\rho^\alpha\left((\vec{r}_1+\vec{r}_2)/2\right)$$

Theoretical Framework

Effective nucleon-nucleon interaction:

Gogny force (D1S) that is able to describe properly many phenomena along the whole nuclear chart.

$$V(1,2) = \sum_{i=1}^{2} e^{-(\vec{r}_1-\vec{r}_2)^2/\mu_i^2} \left(W_i + B_i P^\sigma - H_i P^\tau - M_i P^\sigma P^\tau\right)$$
$$+ iW_0(\sigma_1+\sigma_2)\vec{k} \times \delta(\vec{r}_1-\vec{r}_2)\vec{k} + V_{\mathrm{Coulomb}}(\vec{r}_1,\vec{r}_2)$$

2-body potential

$$+t_3(1+x_0P^\sigma)\delta(\vec{r}_1-\vec{r}_2)\rho^\alpha\left((\vec{r}_1+\vec{r}_2)/2\right)$$

Theoretical Framework

Effective nucleon-nucleon interaction:

Gogny force (D1S) that is able to describe properly many phenomena along the whole nuclear chart.

$$V(1,2)=\sum_{i=1}^{2} e^{-(\vec{r}_1-\vec{r}_2)^2/\mu_i^2}\left(W_i+B_iP^\sigma-H_iP^\tau-M_iP^\sigma P^\tau\right)$$

$$+iW_0(\sigma_1+\sigma_2)\vec{k}\times\delta(\vec{r}_1-\vec{r}_2)\vec{k}+V_{\mathrm{Coulomb}}(\vec{r}_1,\vec{r}_2)$$

2-body potential

$$+t_3(1+x_0P^\sigma)\delta(\vec{r}_1-\vec{r}_2)\rho^\alpha\left((\vec{r}_1+\vec{r}_2)/2\right)$$

Density dependent term

CONTENTS

Theoretical Framework

- **Effective nucleon-nucleon interaction:**

Gogny force (D1S) that is able to describe properly many phenomena along the whole nuclear chart.

$$V(1,2) = \sum_{i=1}^{2} e^{-(\vec{r}_1-\vec{r}_2)^2/\mu_i^2}\left(W_i + B_i P^\sigma - H_i P^\tau - M_i P^\sigma P^\tau\right)$$
$$+iW_0(\sigma_1+\sigma_2)\vec{k}\times\delta(\vec{r}_1-\vec{r}_2)\vec{k} + V_{\mathrm{Coulomb}}(\vec{r}_1,\vec{r}_2)$$

2-body potential

$$+t_3(1+x_0P^\sigma)\delta(\vec{r}_1-\vec{r}_2)\rho^\alpha\left((\vec{r}_1+\vec{r}_2)/2\right)$$

Density dependent term

- **Prescriptions:**

$$\varepsilon_{DD}^{N,Z}(\Phi)$$

$$\rho_H^{NZ}(\vec{r}) \equiv \frac{\langle\Phi|\hat{\rho}(\vec{r})P^N P^Z|\Phi\rangle}{\langle\Phi|P^N P^Z|\Phi\rangle}$$

$$\varepsilon_{DD}^{IKK';NZ}\left[\Phi(\beta,\gamma),\Phi'(\beta',\gamma')\right]$$

$$\rho_H^{NZ}(\Omega,\vec{r}) \equiv \frac{\langle\Phi|\hat{\rho}(\vec{r})\hat{R}(\Omega)P^N P^Z|\Phi'\rangle}{\langle\Phi|\hat{R}(\Omega)P^N P^Z|\Phi'\rangle}$$

Theoretical Framework

CONTENTS

Axial calculations ^{24}Mg

First step: Particle Number Projection (before the variation) of HFB-type wave functions.

$|\Phi(\beta)\rangle$ product-type many body wave function

$$|\Phi^{N,Z}(\beta)\rangle = \hat{P}^N \hat{P}^Z |\Phi(\beta)\rangle$$

$E^{N,Z}(\beta)$ Potential Energy Surface

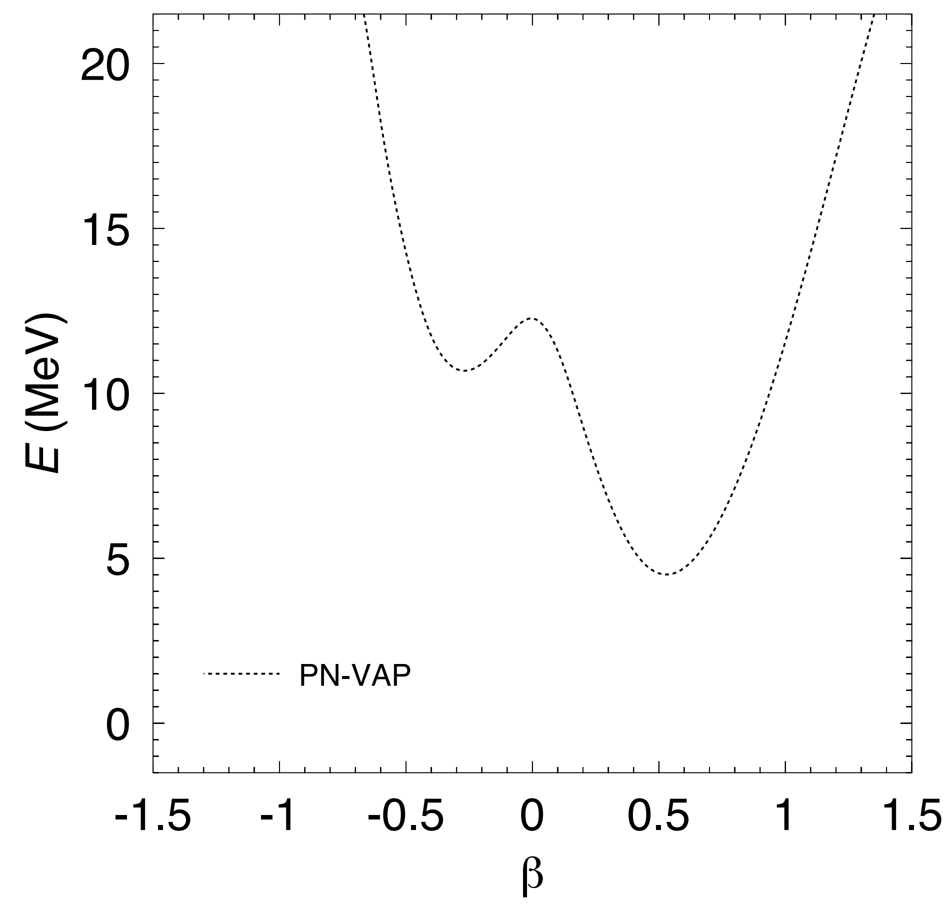

CONTENTS

Theoretical Framework

Axial calculations ^{24}Mg

First step: Particle Number Projection (before the variation) of HFB-type wave functions.

$|\Phi(\beta)\rangle$ product-type many body wave function

$$\Downarrow$$

$$|\Phi^{N,Z}(\beta)\rangle = \hat{P}^N \hat{P}^Z |\Phi(\beta)\rangle$$

$$\Downarrow$$

$E^{N,Z}(\beta)$ Potential Energy Surface

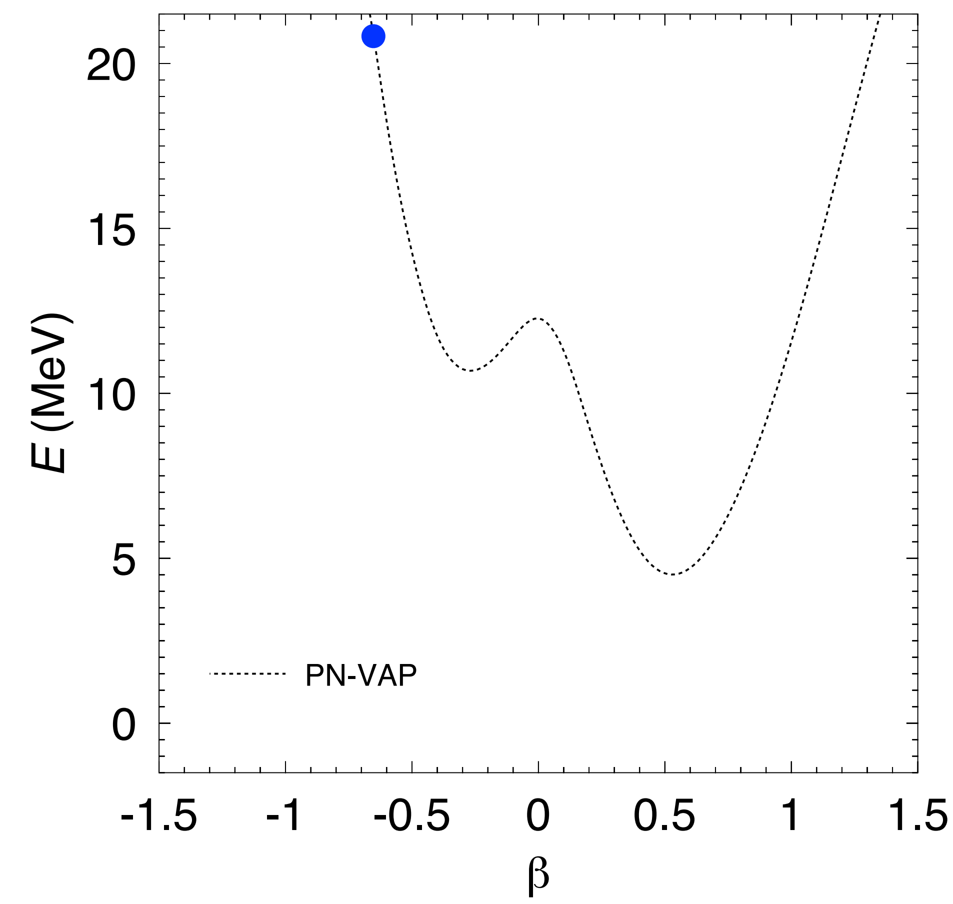

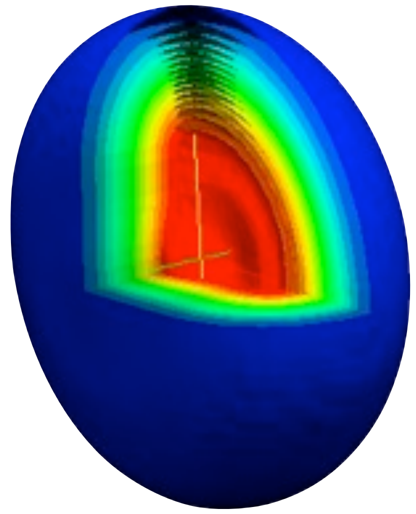

GSI theory HIC for FAIR

CONTENTS

1. Theoretical framework

2. Applications

3. Conclusions and outlook

Theoretical Framework

Axial calculations ^{24}Mg

Second step: Simultaneous **Particle Number and Angular Momentum Projection**

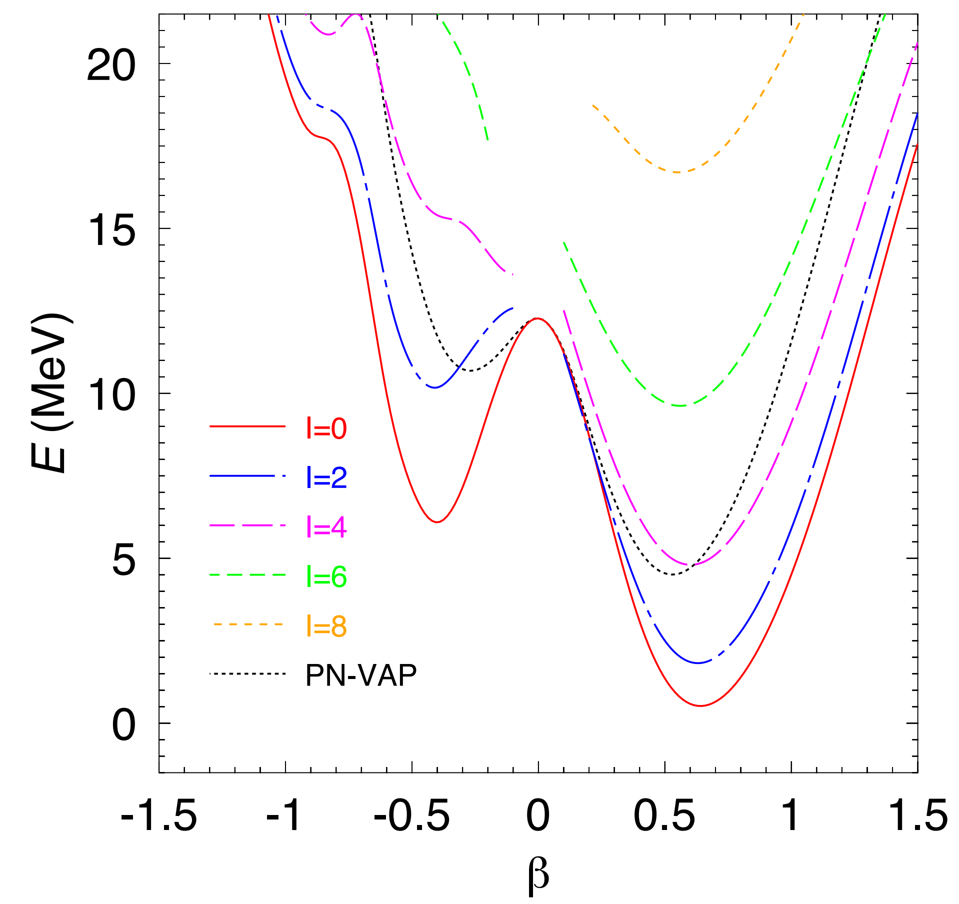

$|\Phi(\beta)\rangle$ product-type many body wave function

$$\Downarrow$$

$$|\Phi^{I,M;N,Z}(\beta)\rangle = \hat{P}^{I}_{00}\hat{P}^{N}\hat{P}^{Z}|\Phi(\beta)\rangle$$

$$\Downarrow$$

$E^{I,N,Z}(\beta)$ Potential Energy Surface

CONTENTS

Theoretical Framework

Axial calculations ^{24}Mg

Third step: Configuration mixing within the framework of the **Generator Coordinate Method (GCM)**.

$$|\Psi^{I;N,Z;\sigma}\rangle = \sum_{\beta} f^{I;N,Z;\sigma}(\beta)\hat{P}^{I}_{00}\hat{P}^{N}\hat{P}^{Z}|\Phi(\beta)\rangle$$

Configuration mixing

$$\sum_{\beta'}\left(\mathcal{H}^{I;NZ}_{\beta\beta'} - E^{I;NZ;\sigma}\mathcal{N}^{I;NZ}_{\beta\beta'}\right) f^{I;NZ;\sigma}_{\beta'} = 0$$

$$\mathcal{N}^{I;NZ}_{\beta\beta'} \equiv \langle\Phi(\beta)|P^{I}_{00}P^{N}P^{Z}|\Phi(\beta')\rangle$$

$$\mathcal{H}^{I;NZ}_{\beta\beta'} \equiv \langle\Phi(\beta)|\hat{H}_{2b}P^{I}_{00}P^{N}P^{Z}|\Phi(\beta')\rangle + \varepsilon^{I;NZ}_{DD}\left[\Phi(\beta),\Phi'(\beta')\right]$$

Hill-Wheeler-Griffin equations

- Energy spectrum
- Observables (mass, radius, B(E2), etc.)
- "Collective w.f."

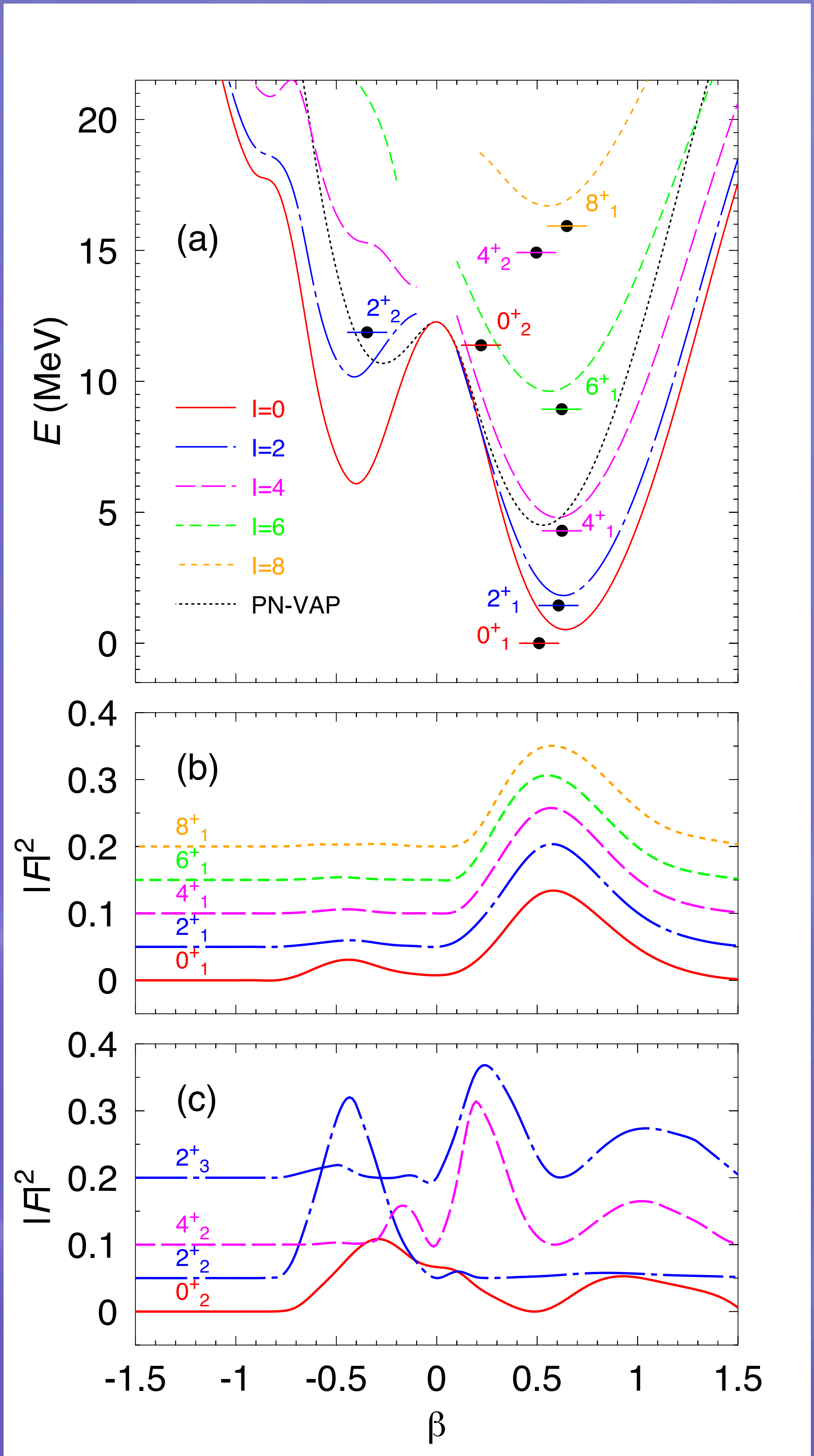

Theoretical Framework

CONTENTS

Triaxiality in nuclei

- Gamma bands and gamma softness in the low energy spectra
- Shape coexistence and/or shape transitions in transitional regions
- Impact of triaxiality in the mass
- Impact of triaxiality in the fission barriers
- Triaxiality at high spin
- ...

CONTENTS

Theoretical Framework

First step: Particle Number Projection (before the variation) of HFB-type wave functions.

$$\delta E^{N,Z}\left[\bar{\Phi}(\beta,\gamma)\right]\Big|_{\bar{\Phi}=\Phi}=0 \quad E^{N,Z}[\Phi]=\frac{\langle\Phi|\hat{H}_{2b}\hat{P}^N\hat{P}^Z|\Phi\rangle}{\langle\Phi|\hat{P}^N\hat{P}^Z|\Phi\rangle}+\varepsilon_{DD}^{N,Z}(\Phi)-\lambda_{q_{20}}\langle\Phi|\hat{Q}_{20}|\Phi\rangle-\lambda_{q_{22}}\langle\Phi|\hat{Q}_{22}|\Phi\rangle$$

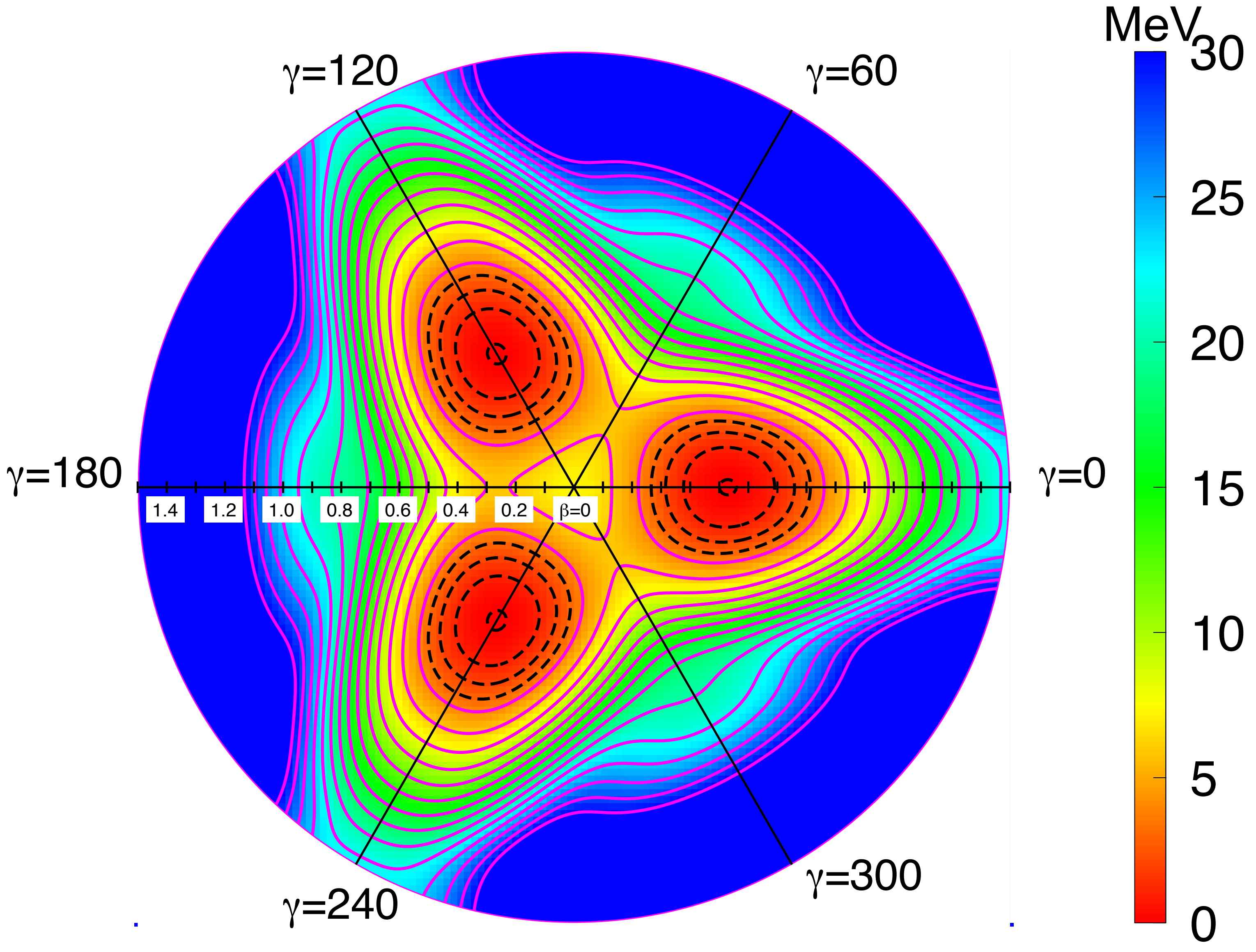

- Symmetry corresponding to the different orientation of the axes
- All configurations are included between γ∈[0º,60º]

Theoretical Framework

First step: Particle Number Projection (before the variation) of HFB-type wave functions.

$$\delta E^{N,Z}\left[\bar{\Phi}(\beta,\gamma)\right]\Big|_{\bar{\Phi}=\Phi}=0 \qquad E^{N,Z}[\Phi]=\frac{\langle\Phi|\hat{H}_{2b}\hat{P}^{N}\hat{P}^{Z}|\Phi\rangle}{\langle\Phi|\hat{P}^{N}\hat{P}^{Z}|\Phi\rangle}+\varepsilon_{DD}^{N,Z}(\Phi)-\lambda_{q_{20}}\langle\Phi|\hat{Q}_{20}|\Phi\rangle-\lambda_{q_{22}}\langle\Phi|\hat{Q}_{22}|\Phi\rangle$$

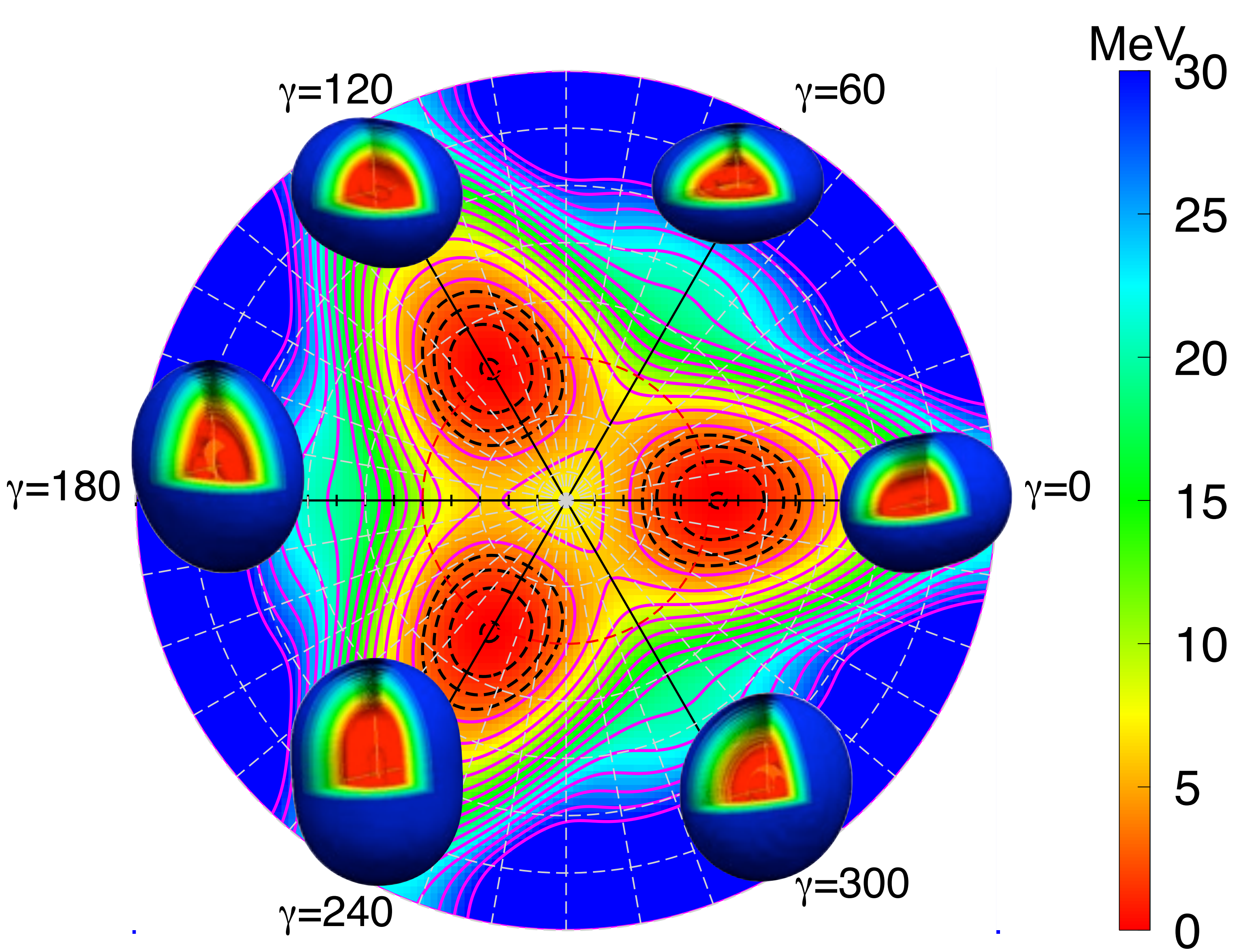

- Symmetry corresponding to the different orientation of the axes
- All configurations are included between γ∈[0º,60º]

CONTENTS

Theoretical Framework

First step: Particle Number Projection (before the variation) of HFB-type wave functions.

$$\delta E^{N,Z}\left[\bar{\Phi}(\beta,\gamma)\right]\Big|_{\bar{\Phi}=\Phi}=0 \qquad E^{N,Z}[\Phi]=\frac{\langle\Phi|\hat{H}_{2b}\hat{P}^{N}\hat{P}^{Z}|\Phi\rangle}{\langle\Phi|\hat{P}^{N}\hat{P}^{Z}|\Phi\rangle}+\varepsilon_{DD}^{N,Z}(\Phi)-\lambda_{q_{20}}\langle\Phi|\hat{Q}_{20}|\Phi\rangle-\lambda_{q_{22}}\langle\Phi|\hat{Q}_{22}|\Phi\rangle$$

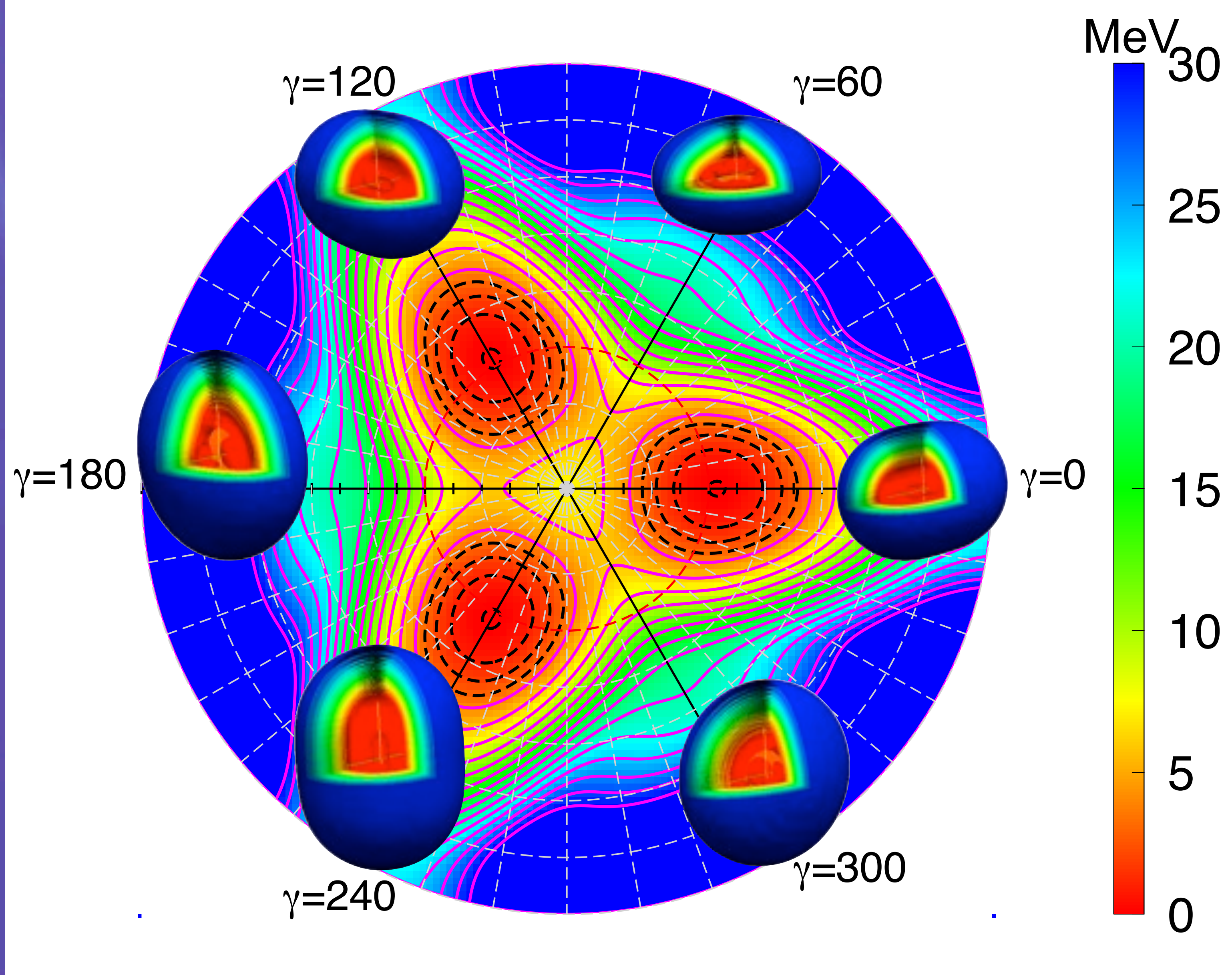

- Symmetry corresponding to the different orientation of the axes
- All configurations are included between γ∈[0º,60º]

CONTENTS

Theoretical Framework

First step: Particle Number Projection (before the variation) of HFB-type wave functions.

$$\delta E^{N,Z}\left[\bar{\Phi}(\beta,\gamma)\right]\Big|_{\bar{\Phi}=\Phi}=0 \qquad E^{N,Z}[\Phi]=\frac{\langle\Phi|\hat{H}_{2b}\hat{P}^{N}\hat{P}^{Z}|\Phi\rangle}{\langle\Phi|\hat{P}^{N}\hat{P}^{Z}|\Phi\rangle}+\varepsilon_{DD}^{N,Z}(\Phi)-\lambda_{q_{20}}\langle\Phi|\hat{Q}_{20}|\Phi\rangle-\lambda_{q_{22}}\langle\Phi|\hat{Q}_{22}|\Phi\rangle$$

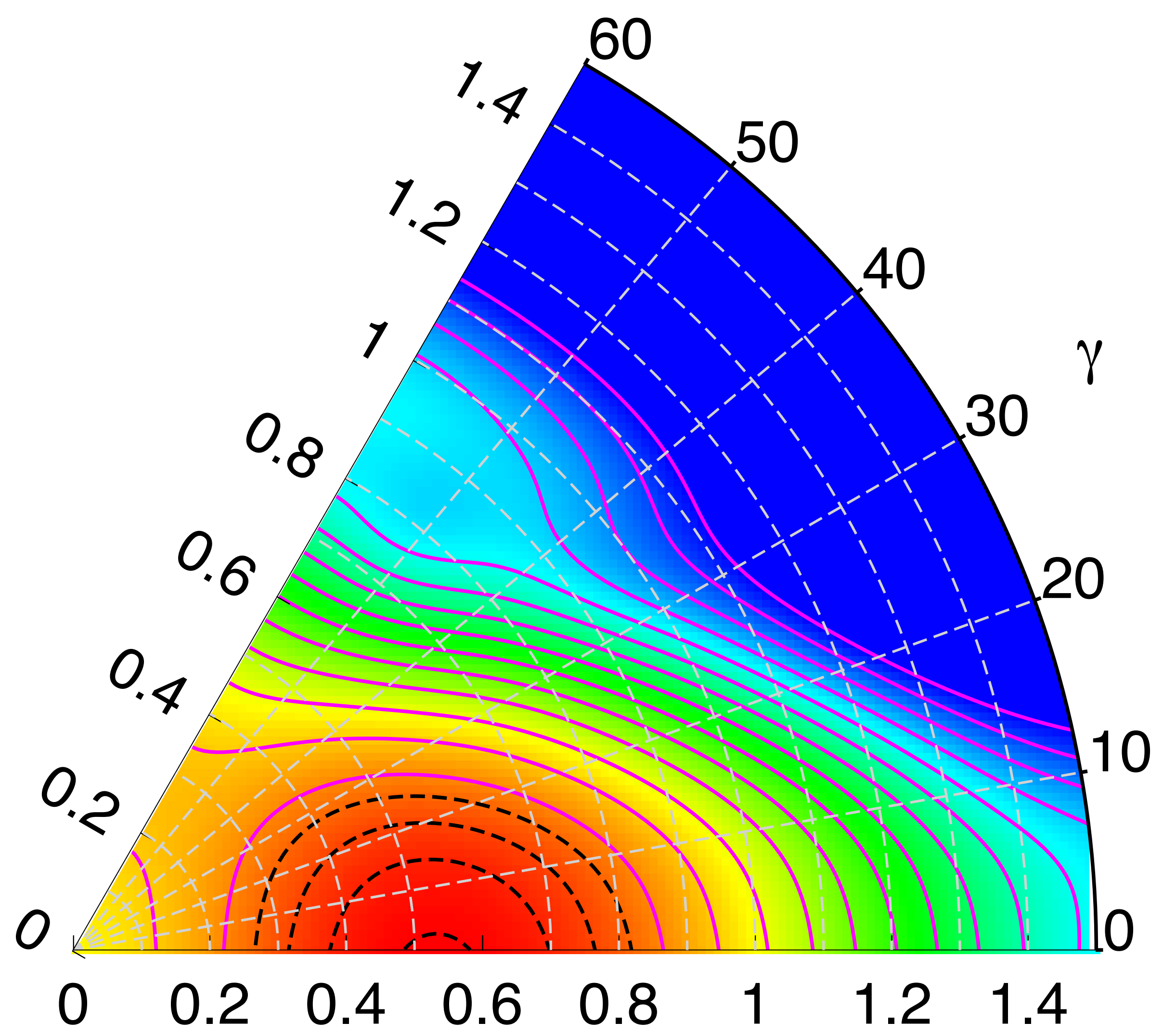

- Symmetry corresponding to the different orientation of the axes
- All configurations are included between γ∈[0º,60º]

Theoretical Framework

Second step: Simultaneous **Particle Number and Angular Momentum Projection**

$$|IMK;NZ;\beta\gamma\rangle = \frac{2I+1}{8\pi^2}\int \mathcal{D}^{I*}_{MK}(\Omega)\hat{R}(\Omega)\hat{P}^N\hat{P}^Z|\Phi(\beta,\gamma)\rangle d\Omega$$

Convergence in Euler angles I

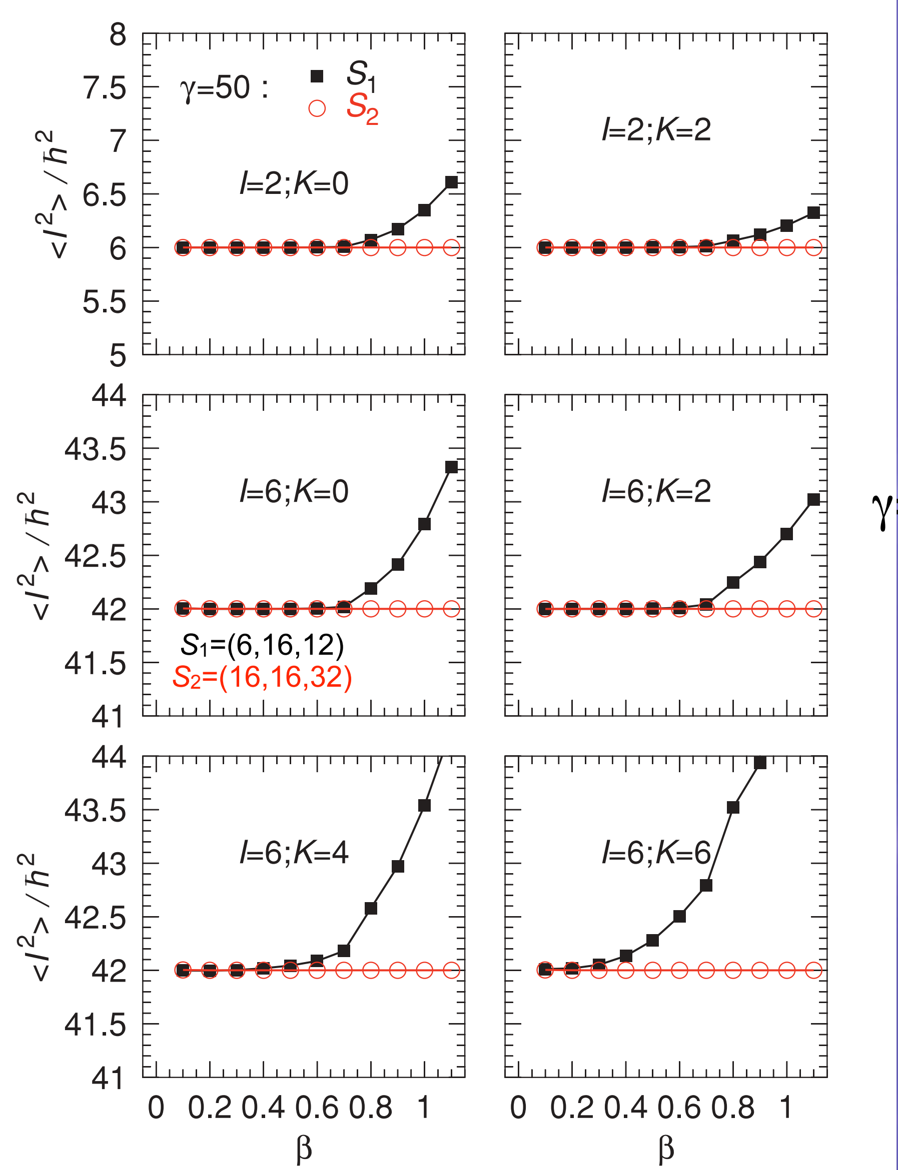

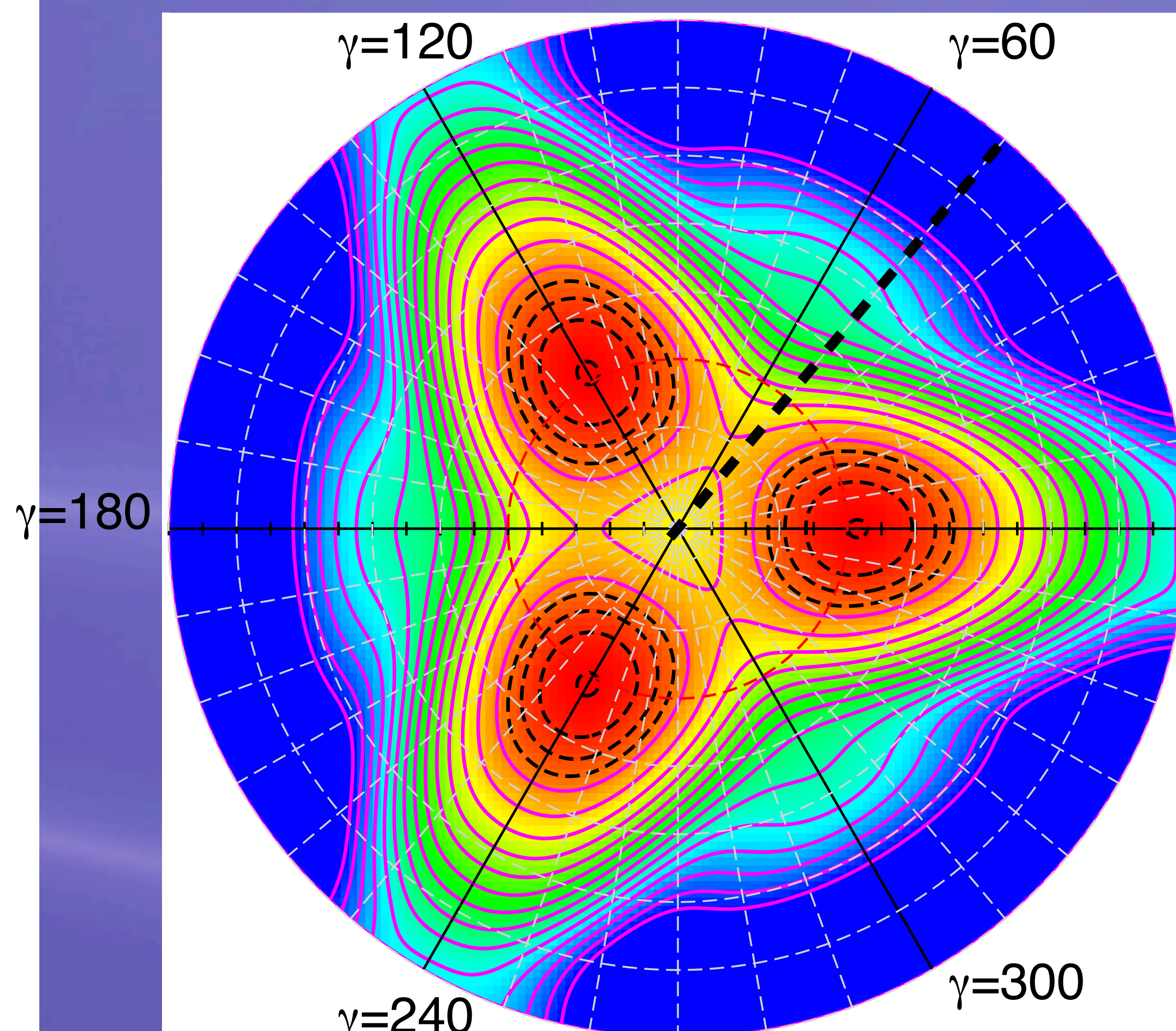

Theoretical Framework

Second step: Simultaneous **Particle Number and Angular Momentum Projection**

$$|IMK;NZ;\beta\gamma\rangle = \frac{2I+1}{8\pi^2}\int \mathcal{D}^{I*}_{MK}(\Omega)\hat{R}(\Omega)\hat{P}^N\hat{P}^Z|\Phi(\beta,\gamma)\rangle d\Omega$$

Convergence in Euler angles II

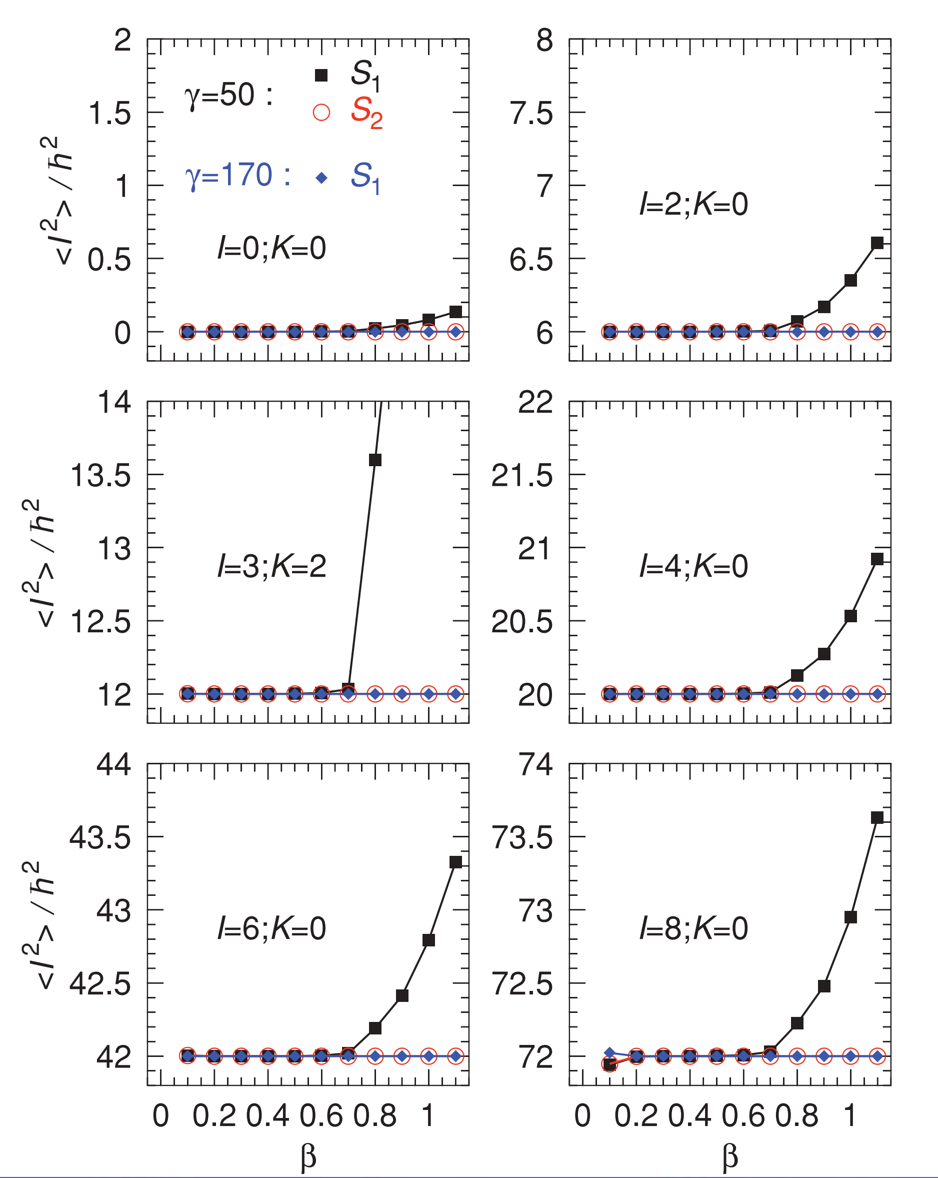

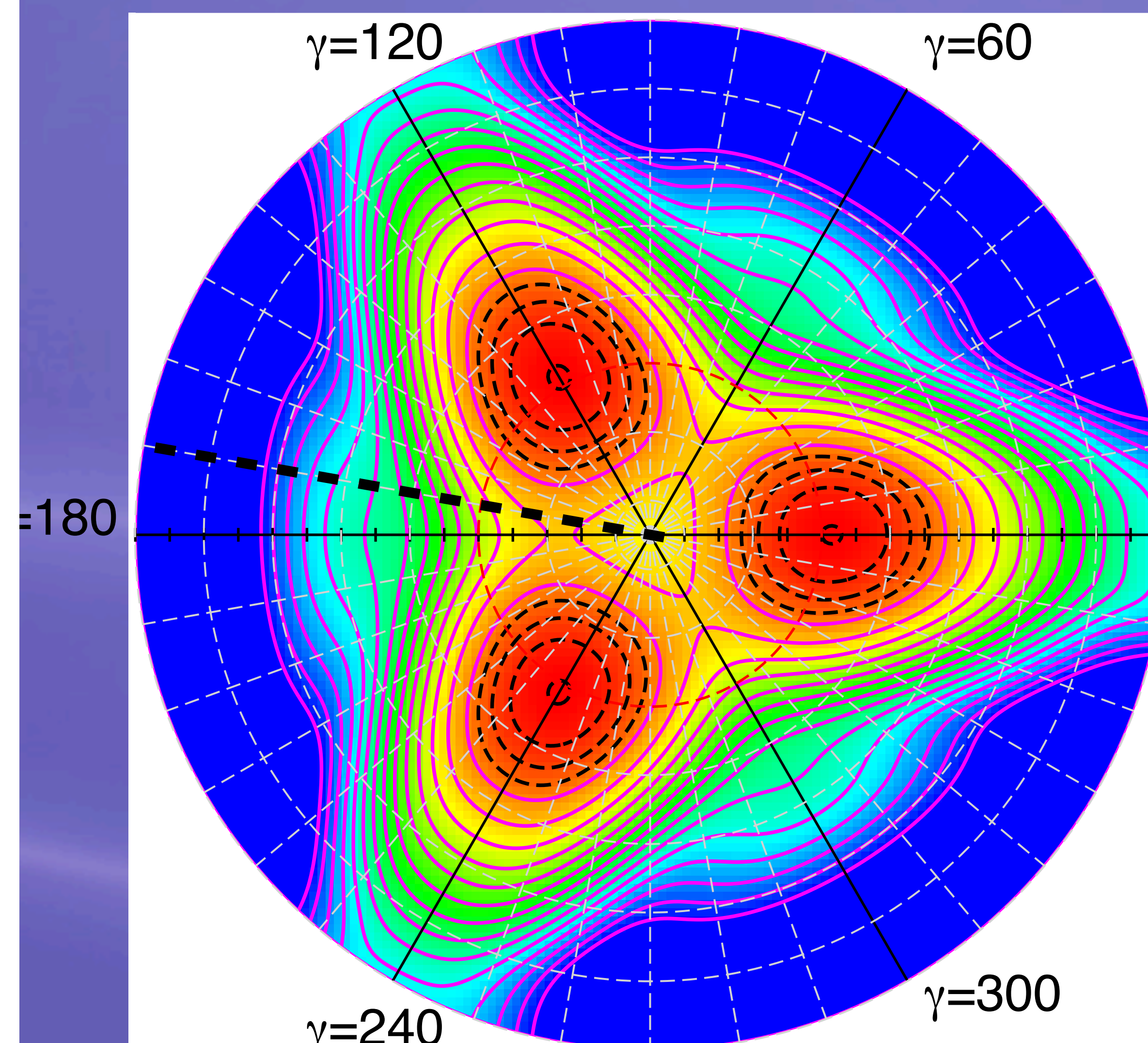

CONTENTS

Theoretical Framework

Second step: Simultaneous **Particle Number and Angular Momentum Projection**

$$|IMK;NZ;\beta\gamma\rangle = \frac{2I+1}{8\pi^2}\int \mathcal{D}^{I*}_{MK}(\Omega)\hat{R}(\Omega)\hat{P}^N\hat{P}^Z|\Phi(\beta,\gamma)\rangle d\Omega$$

$$|IM;NZ;\beta\gamma\rangle = \sum_K g_K^{IM;NZ;\beta\gamma}|IMK;NZ;\beta\gamma\rangle$$

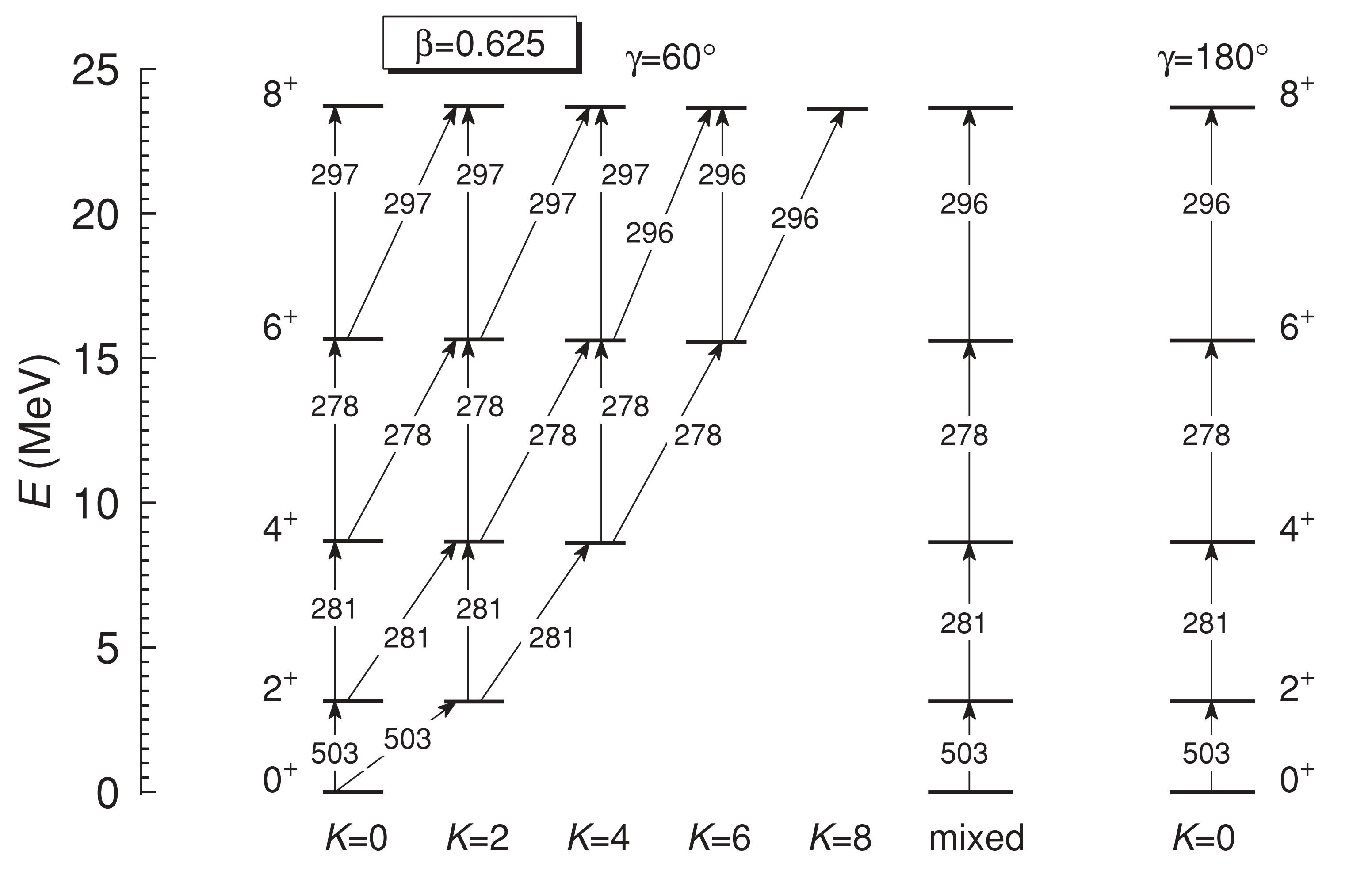

K-mixing and consistency I

Theoretical Framework

Second step: Simultaneous **Particle Number and Angular Momentum Projection**

$$|IMK;NZ;\beta\gamma\rangle = \frac{2I+1}{8\pi^2}\int \mathcal{D}^{I*}_{MK}(\Omega)\hat{R}(\Omega)\hat{P}^N\hat{P}^Z|\Phi(\beta,\gamma)\rangle d\Omega$$

$$|IM;NZ;\beta\gamma\rangle = \sum_K g_K^{IM;NZ;\beta\gamma}|IMK;NZ;\beta\gamma\rangle$$

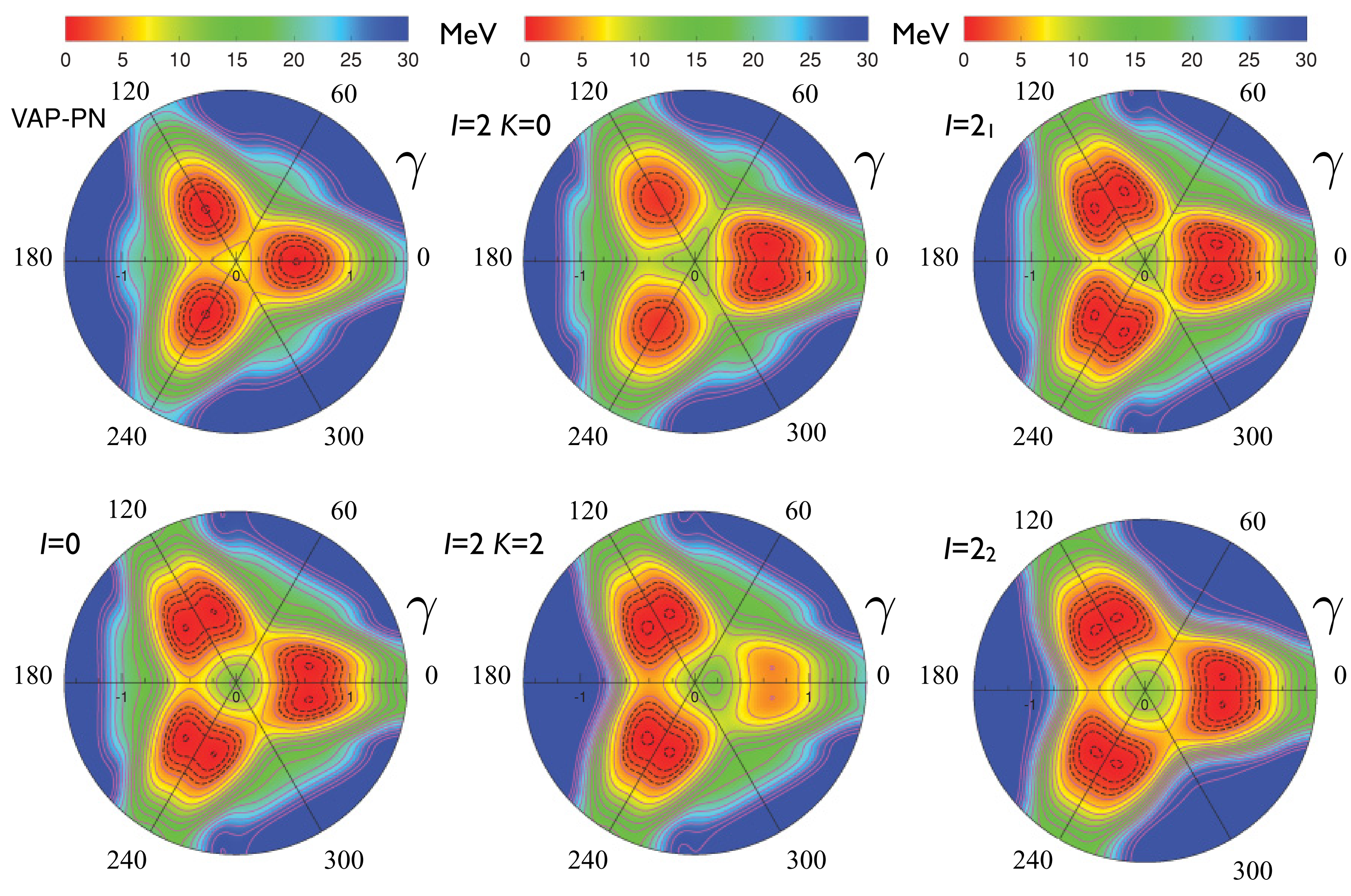

K-mixing and consistency II

PES without *K*-mixing depend on the orientation of the reference frame!

CONTENTS

CONTENTS

Theoretical Framework

Triaxial calculations ^{24}Mg

Second step: Simultaneous **Particle Number and Angular Momentum Projection**

$$|IMK;NZ;\beta\gamma\rangle = \frac{2I+1}{8\pi^2}\int \mathcal{D}^{I*}_{MK}(\Omega)\hat{R}(\Omega)\hat{P}^N\hat{P}^Z|\Phi(\beta,\gamma)\rangle d\Omega$$

$$|IM;NZ;\beta\gamma\rangle = \sum_K g_K^{IM;NZ;\beta\gamma}|IMK;NZ;\beta\gamma\rangle$$

- Minimum displaced to triaxial shapes.

- Projection onto odd *I* angular momentum

-Softening of PES with increasing *I*.

- Difference between triaxial minimum and axial saddle point of ~ 0.7 MeV (0^+)

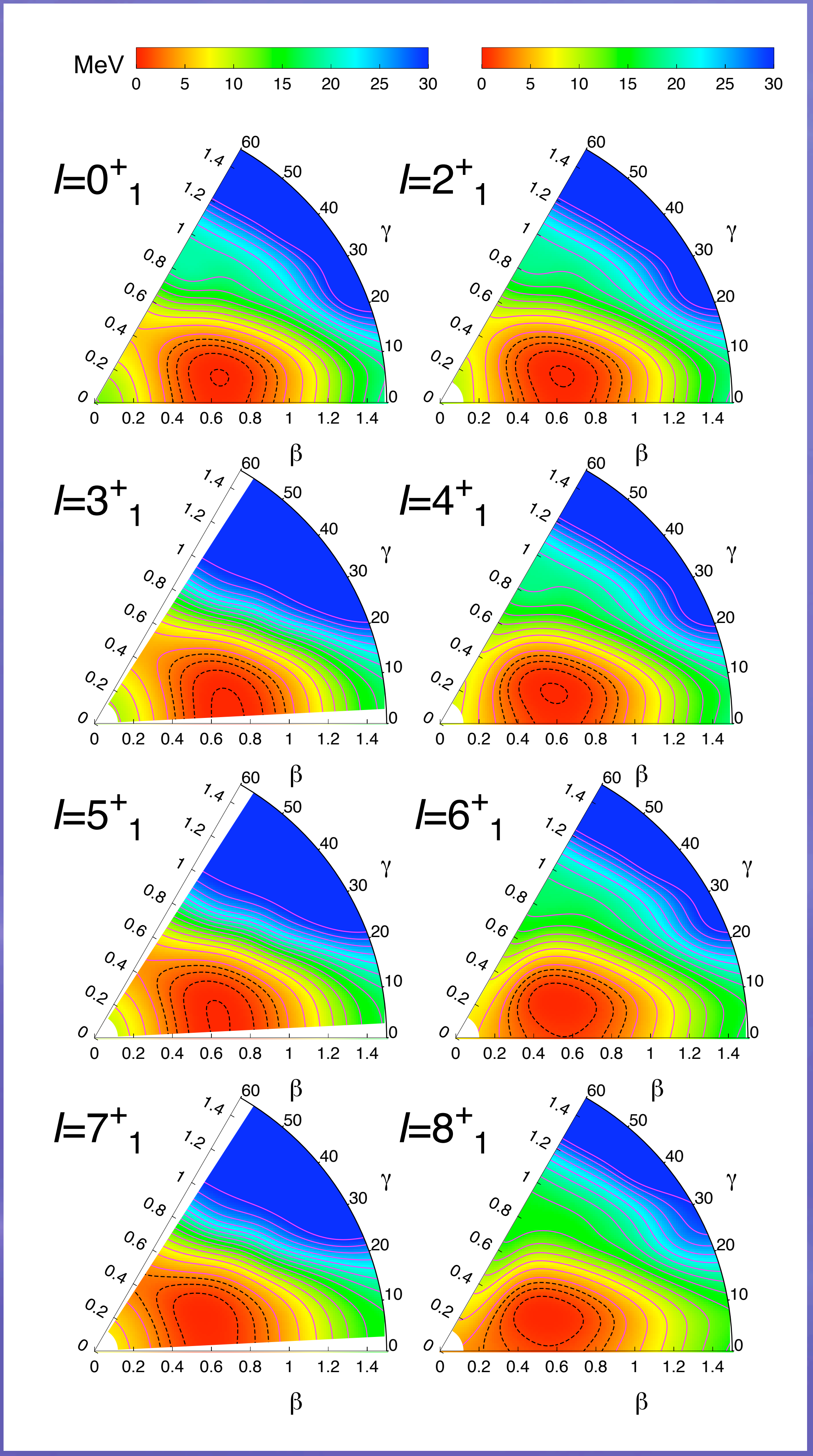

Theoretical Framework

Third step: Configuration mixing within the framework of the **Generator Coordinate Method (GCM)**. ***K* and deformation mixing**

Selection of the mesh. Resolution.

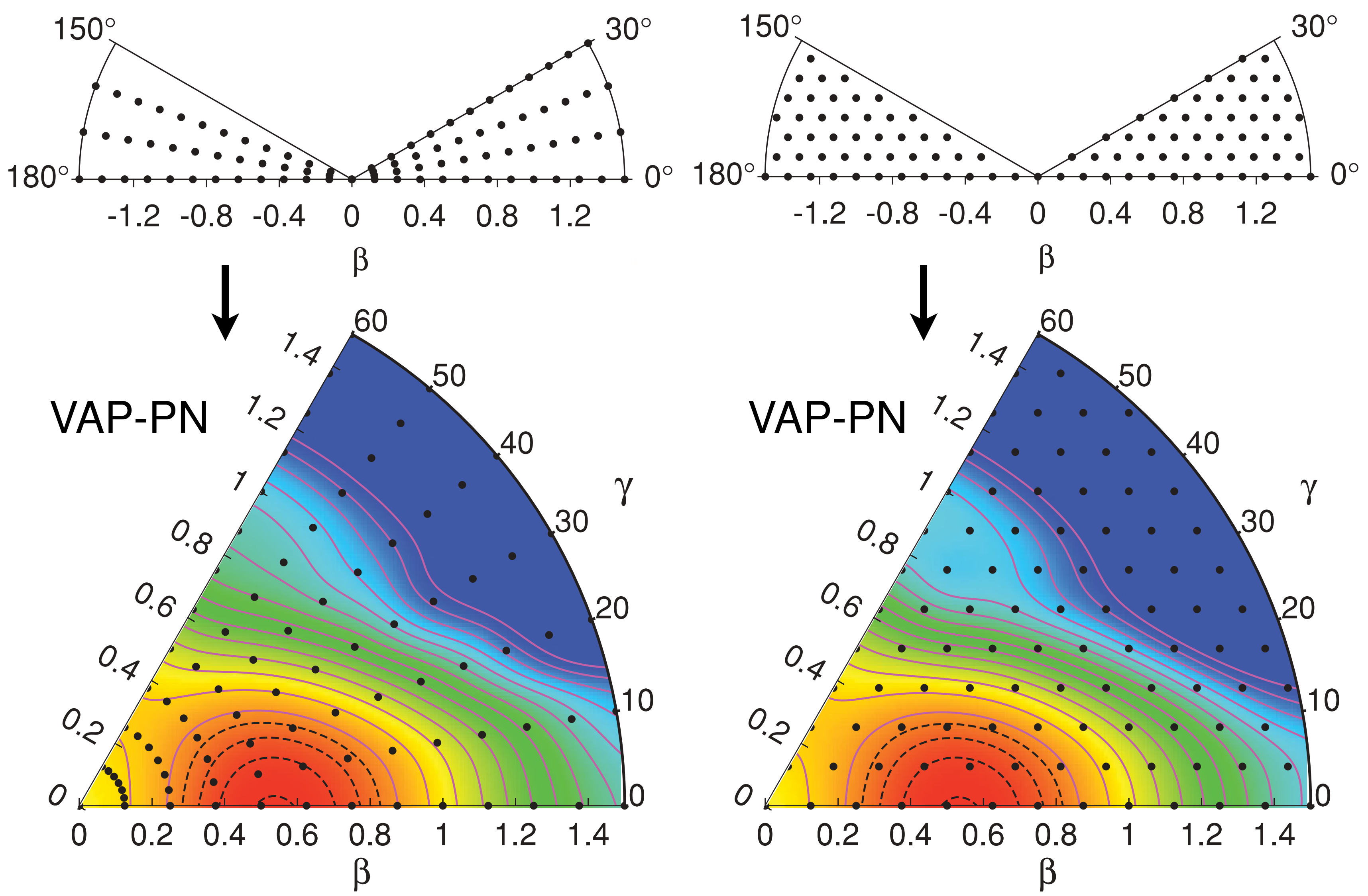

CONTENTS

Theoretical Framework

Third step: Configuration mixing within the framework of the **Generator Coordinate Method (GCM)**. ***K* and deformation mixing**

Selection of the mesh. Resolution.

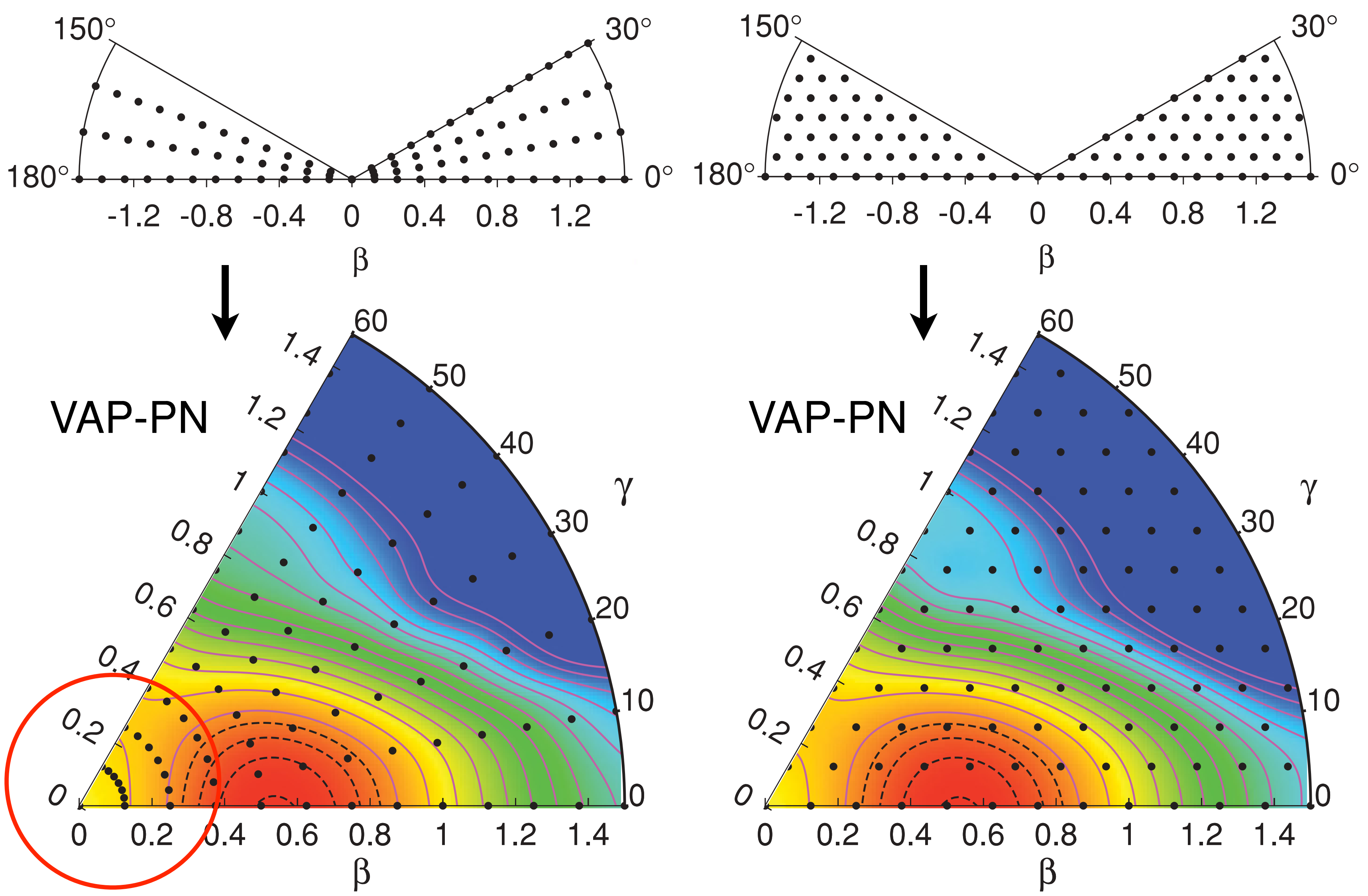

Theoretical Framework

Third step: Configuration mixing within the framework of the **Generator Coordinate Method (GCM)**. ***K* and deformation mixing**

CONTENTS

Selection of the mesh. Resolution.

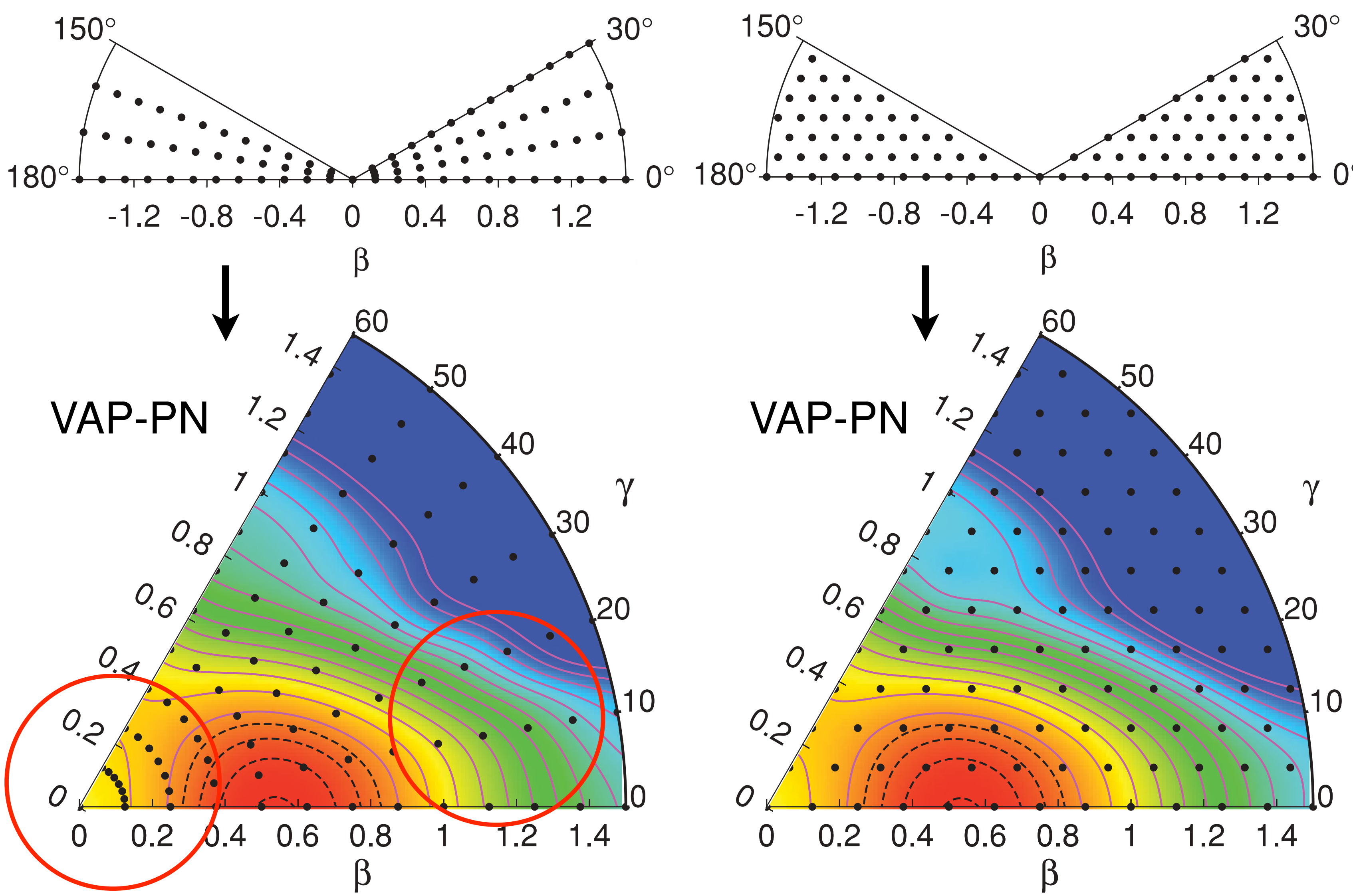

Theoretical Framework

Third step: Configuration mixing within the framework of the **Generator Coordinate Method (GCM)**. ***K* and deformation mixing**

CONTENTS

Selection of the mesh. Resolution.

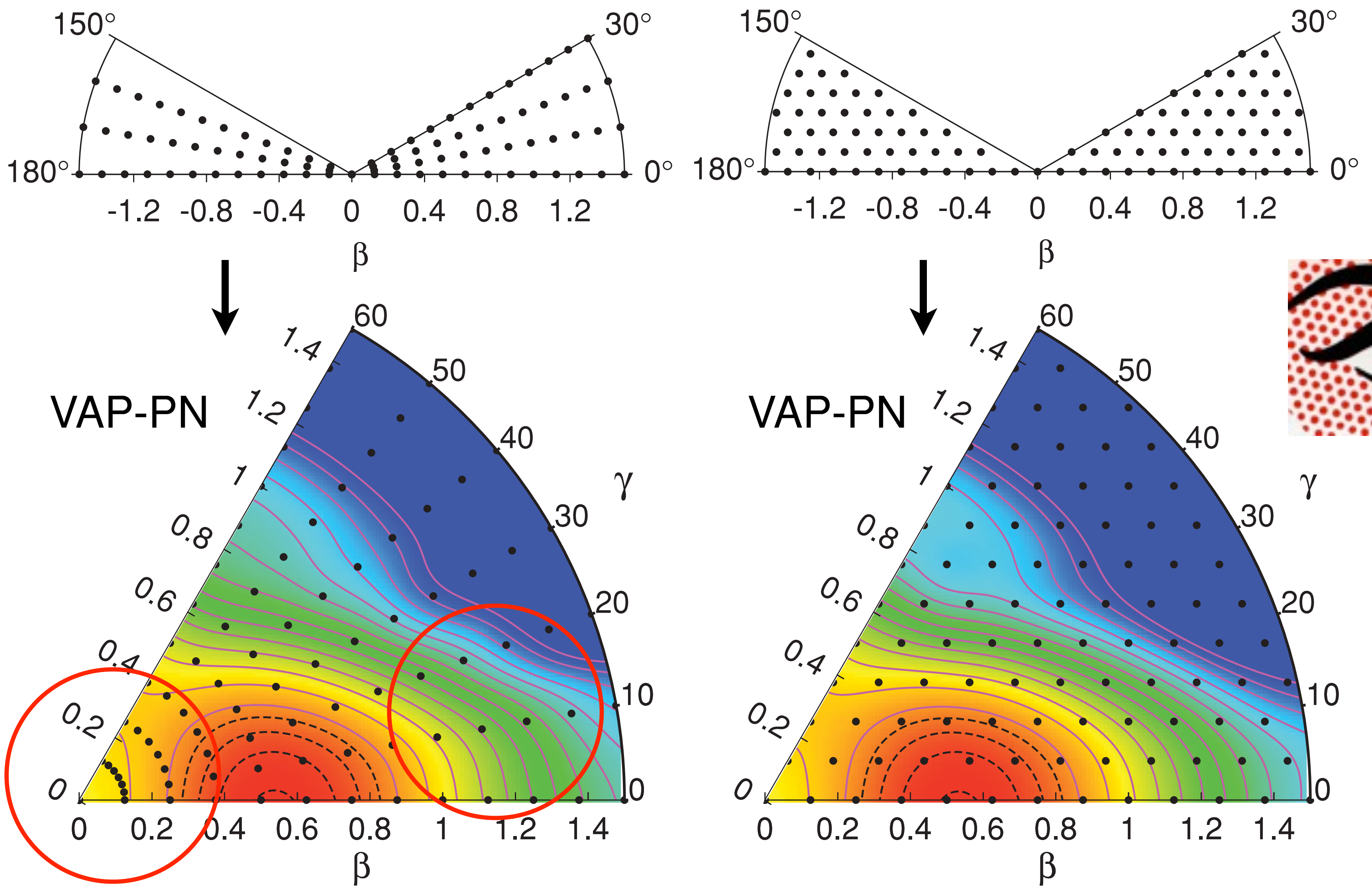

CONTENTS

Theoretical Framework

Third step: Configuration mixing within the framework of the **Generator Coordinate Method (GCM)**. ***K* and deformation mixing**

$$|IM;NZ\sigma\rangle = \sum_{K\beta\gamma} f^{I;NZ,\sigma}_{K\beta\gamma} |IMK;NZ;\beta\gamma\rangle$$

$$\sum_{K'\beta'\gamma'} \left(\mathcal{H}^{I;NZ}_{K\beta\gamma K'\beta'\gamma'} - E^{I;NZ;\sigma}\mathcal{N}^{I;NZ}_{K\beta\gamma K'\beta'\gamma'}\right) f^{I;NZ;\sigma}_{K'\beta'\gamma'} = 0$$

Convergence of the GCM states

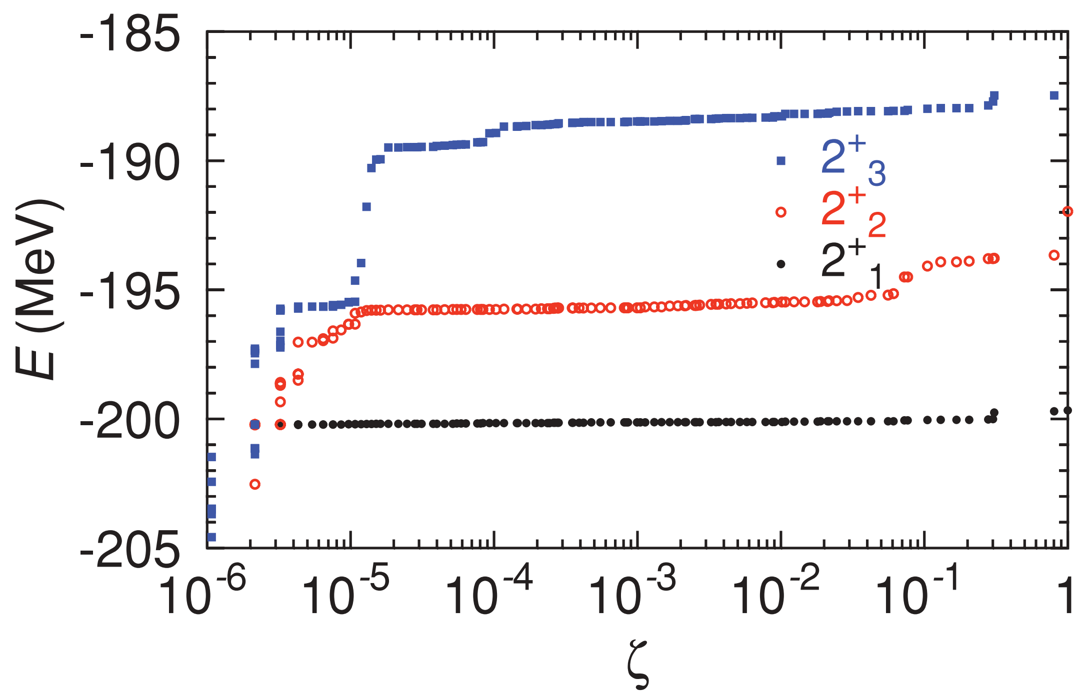

- Plateau condition as a function of natural states.

- Orthogonalization requirements.

CONTENTS

1. Theoretical framework

2. Applications

3. ...

Theoretical Framework

Third step: Configuration mixing within the framework of the **Generator Coordinate Method (GCM)**. ***K* and deformation mixing**

- Axial ground state rotational band well described with axial calculations in this nucleus

- Second band associated to a gamma band

- Overall qualitative agreement between experimental data and triaxial calculations (energies and B(E2))

- Too high energies for the second and third band heads (lack of time reversal symmetry broken -cranking- states)

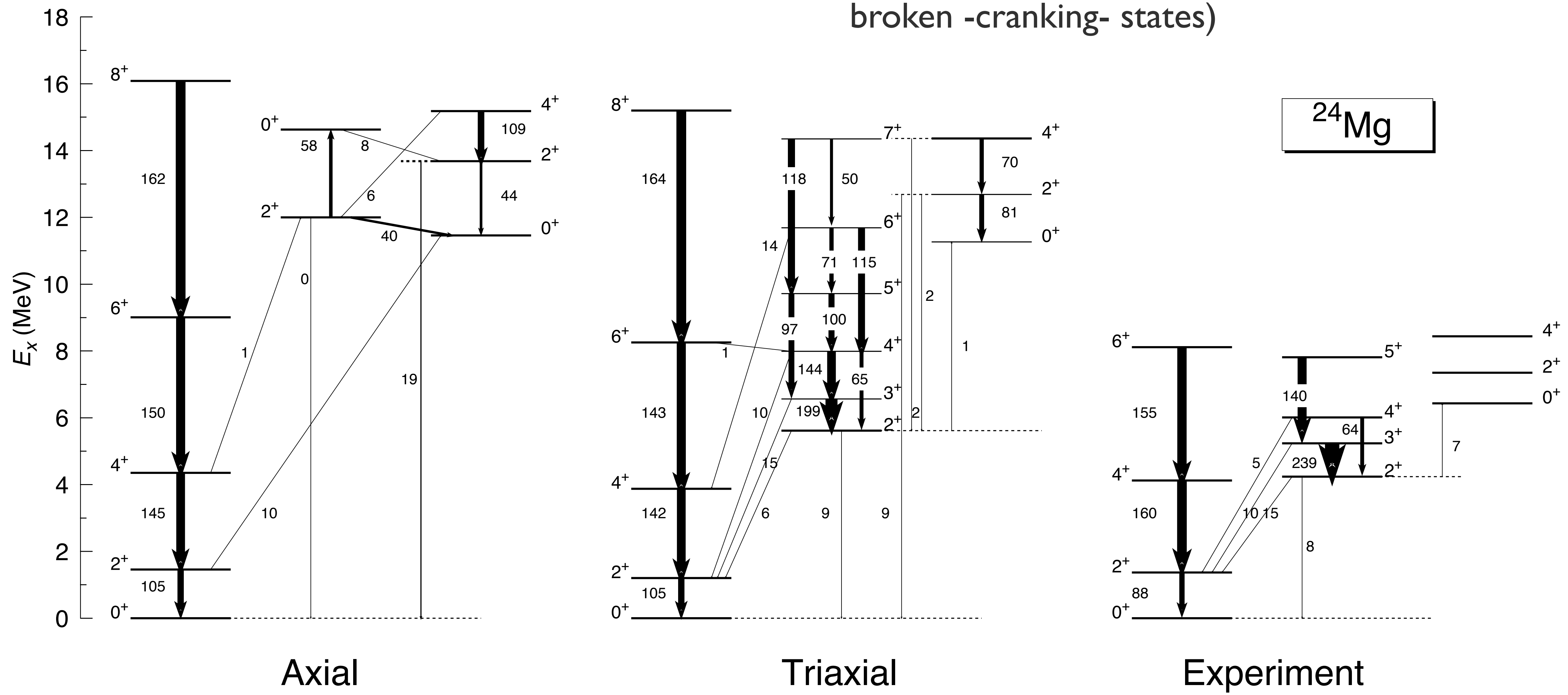

Theoretical Framework

Third step: Configuration mixing within the framework of the **Generator Coordinate Method (GCM)**. ***K* and deformation mixing**

$$|IM;NZ\sigma\rangle = \sum_{K\beta\gamma} f^{I;NZ,\sigma}_{K\beta\gamma} |IMK;NZ;\beta\gamma\rangle$$

$$\sum_{K'\beta'\gamma'} \left(\mathcal{H}^{I;NZ}_{K\beta\gamma K'\beta'\gamma'} - E^{I;NZ;\sigma}\mathcal{N}^{I;NZ}_{K\beta\gamma K'\beta'\gamma'}\right) f^{I;NZ;\sigma}_{K'\beta'\gamma'} = 0$$

- Axial ground state rotational band

- Second band associated to a gamma band

-Third band with shape mixing

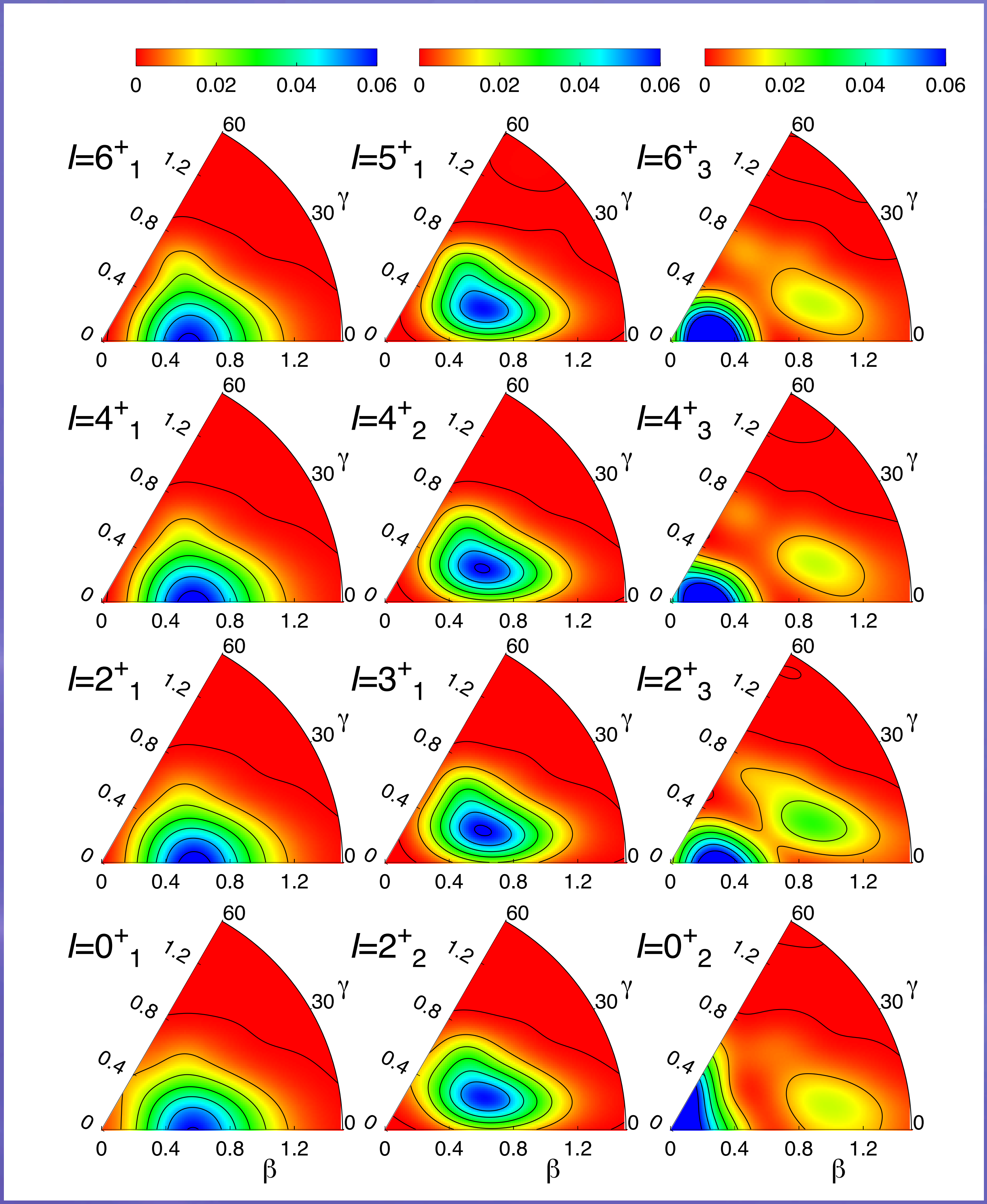

GSI theory HIC for FAIR Helmholtz International Center

CONTENTS

Theoretical Framework

Third step: Configuration mixing within the framework of the **Generator Coordinate Method (GCM)**. ***K* and deformation mixing**

$$|IM;NZ\sigma\rangle = \sum_{K\beta\gamma} f^{I;NZ,\sigma}_{K\beta\gamma}|IMK;NZ;\beta\gamma\rangle$$

$$\sum_{K'\beta'\gamma'}\left(\mathcal{H}^{I;NZ}_{K\beta\gamma K'\beta'\gamma'} - E^{I;NZ;\sigma}\mathcal{N}^{I;NZ}_{K\beta\gamma K'\beta'\gamma'}\right) f^{I;NZ;\sigma}_{K'\beta'\gamma'} = 0$$

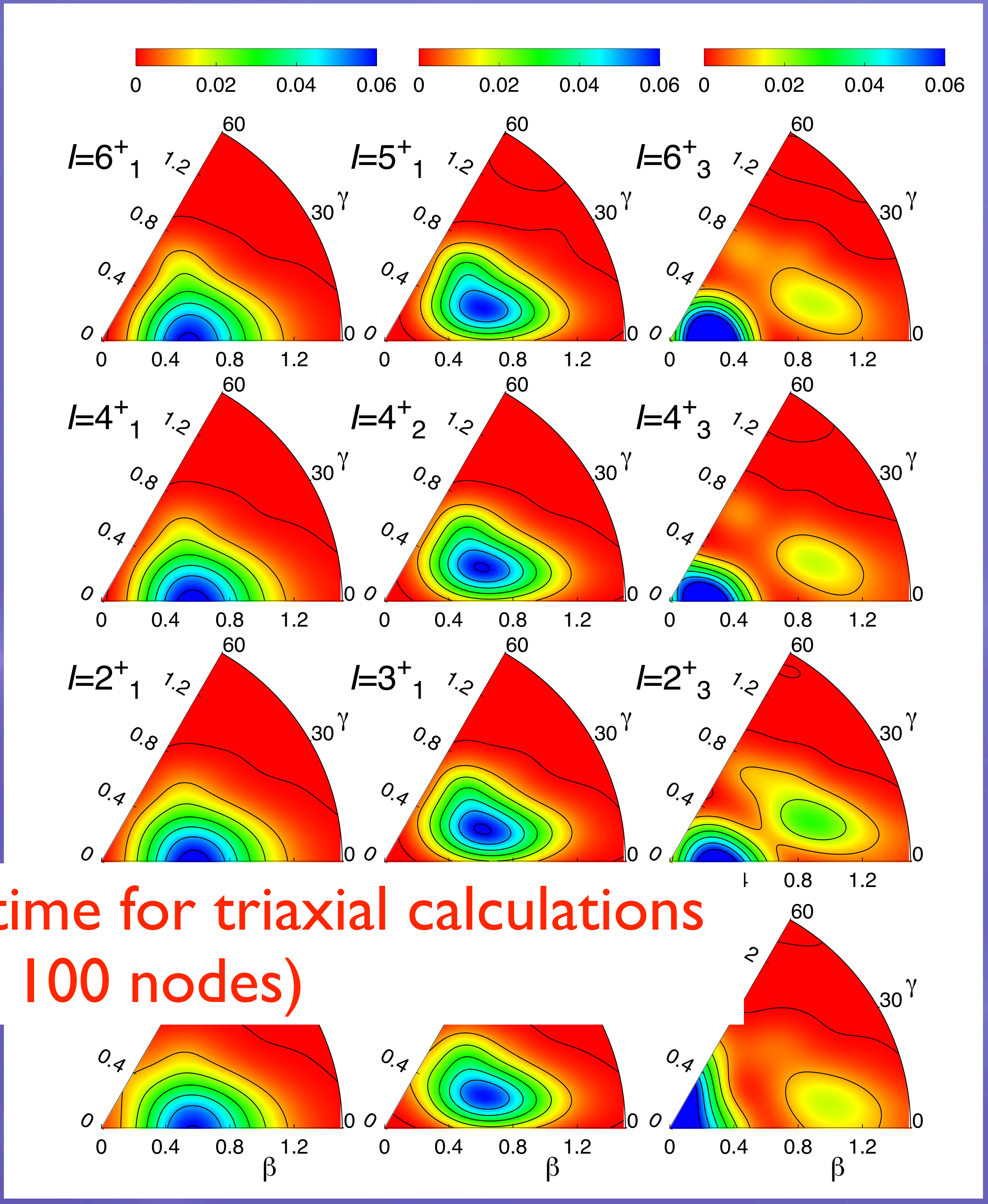

- Axial ground state rotational band

-
ga

-Third band with shape mixing

Problem: Computational time for triaxial calculations (~1 month per nucleus in 100 nodes)

CONTENTS

Theoretical Framework

Recipe for cooking triaxial calculations

- Check the interval of deformations and the number of oscillator shells with axial calculations.

- Use a high resolution mesh in the triaxial plane.

- Check the number of integration points in the Euler angles studying the corresponding known mean values. Use rotated states to improve the convergence.

- Check the convergence of the final GCM calculations (plateau condition and orthonormalization requirements).

Applications

Skyrme: M. Bender, P.-H. Heenen, Phys. Rev. C 78, 024309 (2008)
- Particle number and angular momentum restoration of intrinsic LN states.

Relativistic: J.M. Yao et al., Phys. Rev. C 81, 04431 (2010)
- Angular momentum restoration of intrinsic HFB states.

Gogny: T.R.R., J.L. Egido, Phys. Rev C 81, 064323 (2010)
- Particle number and angular momentum restoration of PN-VAP states.

^{24}Mg is a bad choice to see triaxial effects!!

Relativistic: J.M. Yao et al., Phys. Rev. C 83, 014308 (2011), Phys. Rev. C 84, 024306 (2011)
Gogny: T.R.R. and J.L.E., Journal of Physics: Conference Series INPC (2010),
Phys. Lett. B submitted, Phys. Rev. C submitted.

CONTENTS

The need of triaxiality: ^{126}Xe as an example

Axial calculations ^{126}Xe

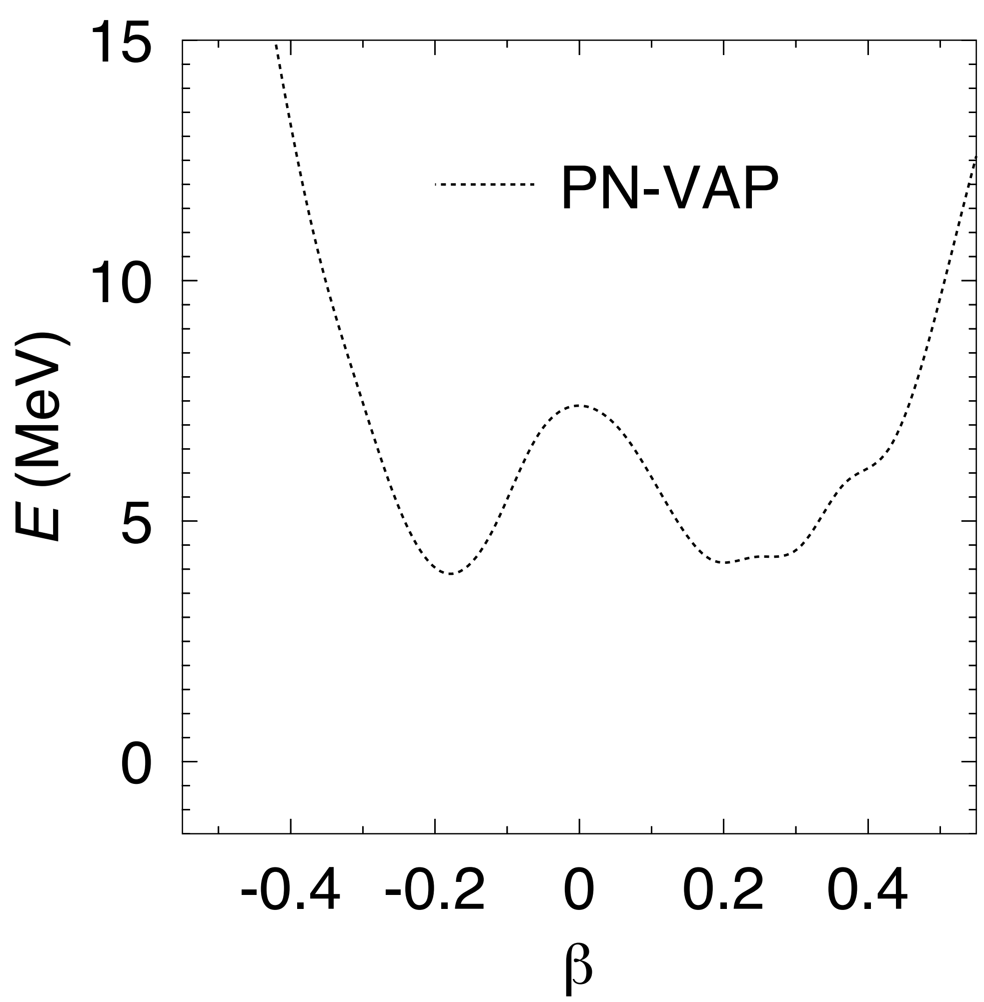

✓ AXIAL calculations

✓ Two minima almost degenerated in the potential energy surface

✓ The collective wave function of the ground state is distributed in these two minima (shape coexistence)

✓ TRIAXIAL calculations?

The need of triaxiality: ^{126}Xe as an example

Axial calculations ^{126}Xe

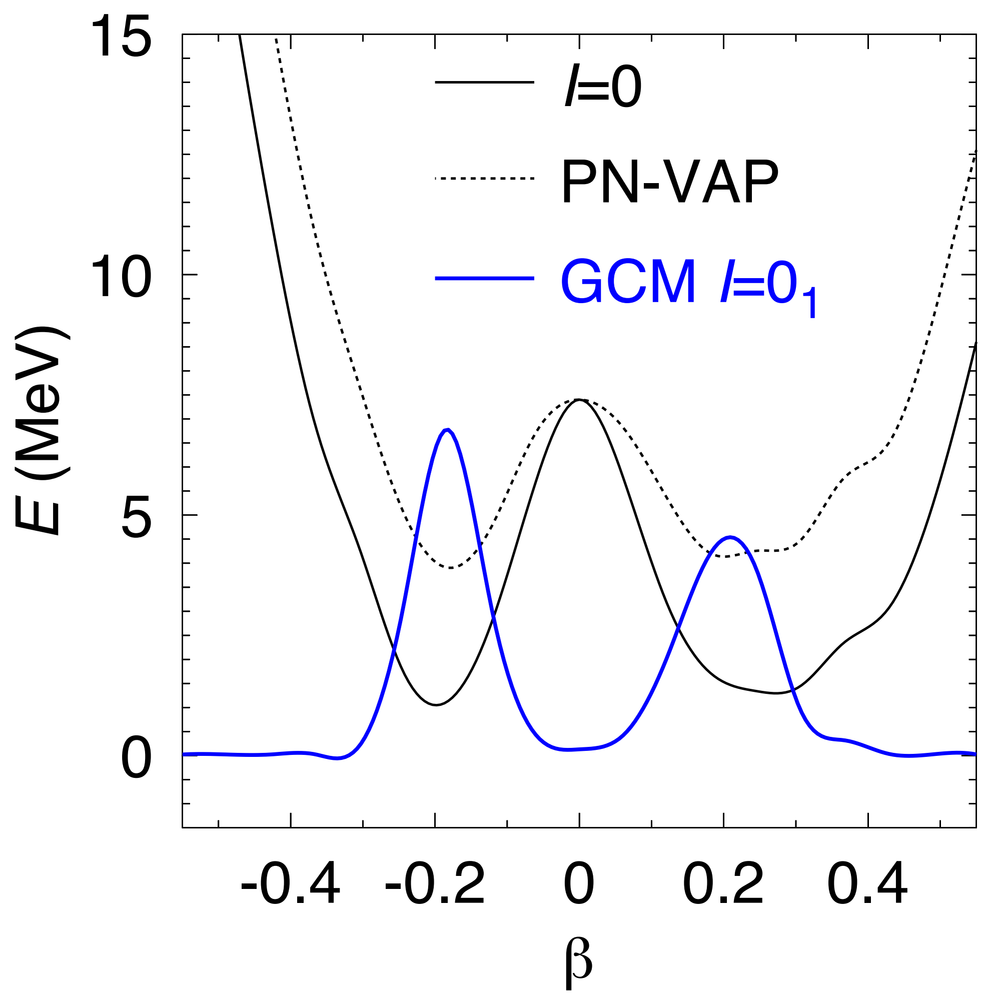

- ✓ AXIAL calculations
- ✓ Two minima almost degenerated in the potential energy surface
- ✓ The collective wave function of the ground state is distributed in these two minima (shape coexistence)
- ✓ TRIAXIAL calculations?

CONTENTS

The need of triaxiality: ^{126}Xe as an example

Triaxial calculations ^{126}Xe in a reduced configuration space (seven shells)

T.R.R and J.L. Egido, Journal of Physics: Conference Series (2011)

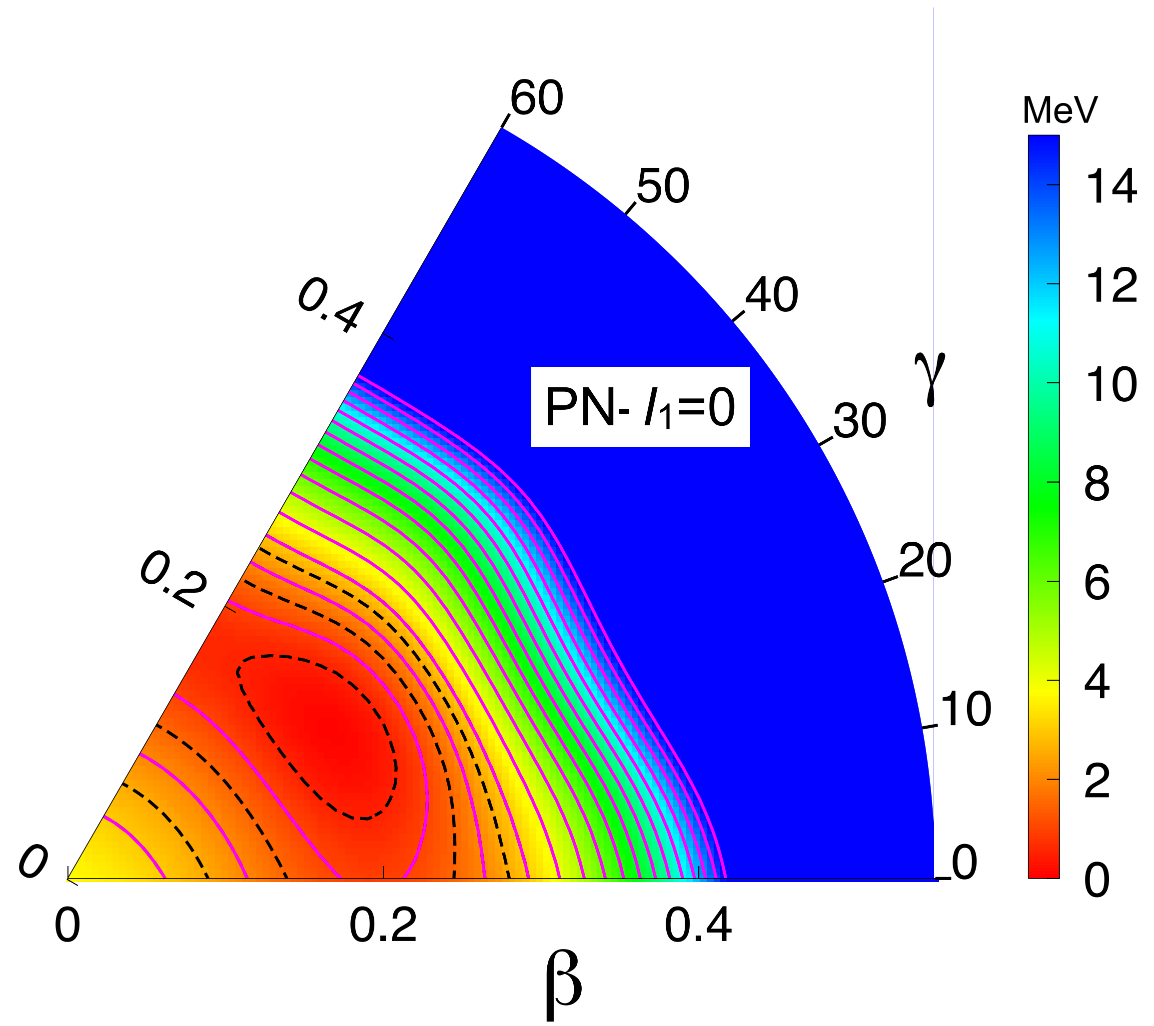

✓ TRIAXIAL calculations

✓ One single minimum in γ=30° and saddle points in the axial configurations

✓ PES very soft in the γ degree of freedom

✓ After GCM, there is not coexistence of prolate and oblate configurations for the ground state, just a triaxial state.

CONTENTS

The need of triaxiality: ^{126}Xe as an example

Triaxial calculations ^{126}Xe in a reduced configuration space (seven shells)

T.R.R and J.L. Egido, Journal of Physics: Conference Series (2011)

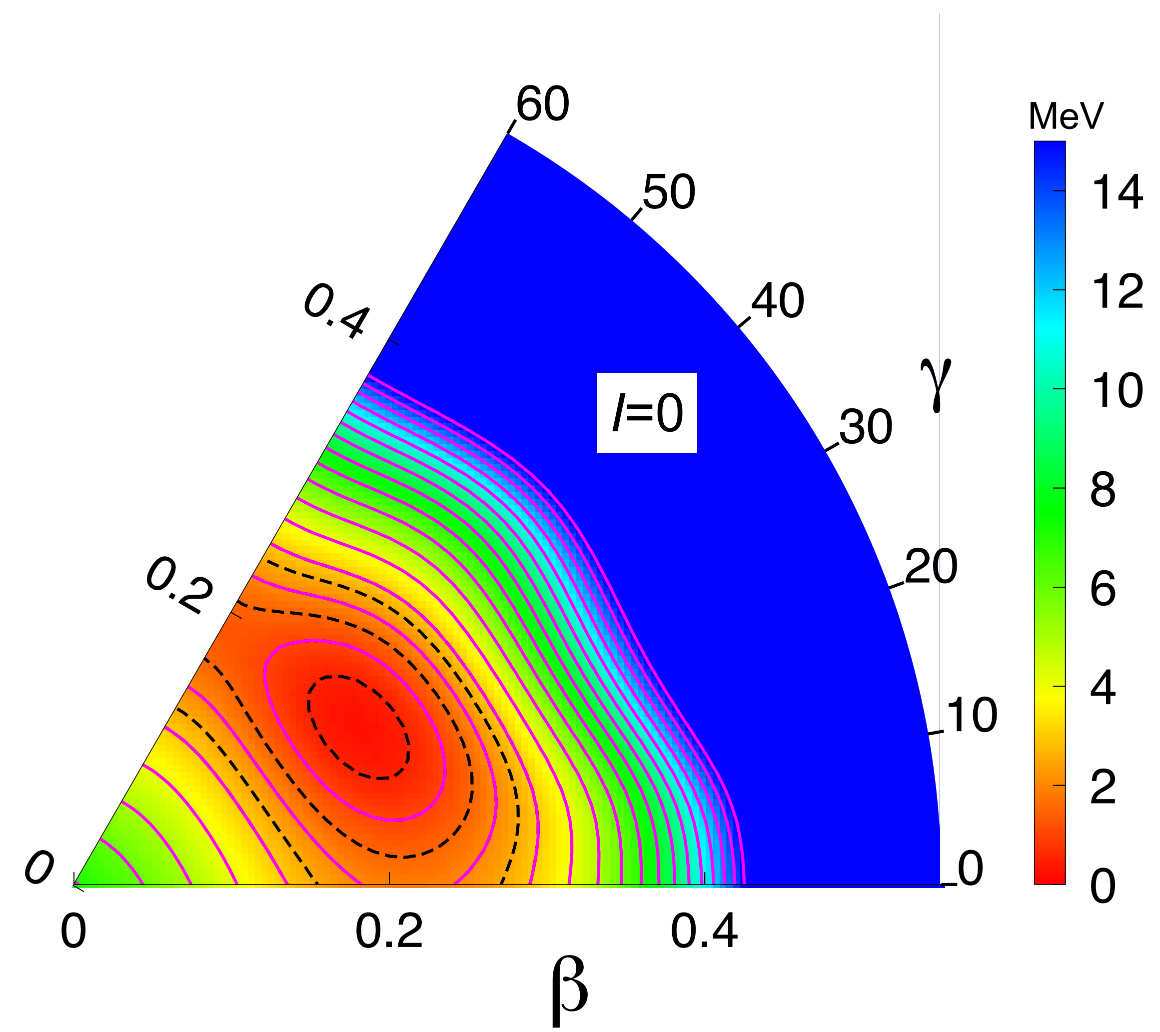

✓ TRIAXIAL calculations

✓ One single minimum in γ=30° and saddle points in the axial configurations

✓ PES very soft in the γ degree of freedom

✓ After GCM, there is not coexistence of prolate and oblate configurations for the ground state, just a triaxial state.

CONTENTS

The need of triaxiality: ^{126}Xe as an example

Triaxial calculations ^{126}Xe in a reduced configuration space (seven shells)

T.R.R and J.L. Egido, Journal of Physics: Conference Series (2011)

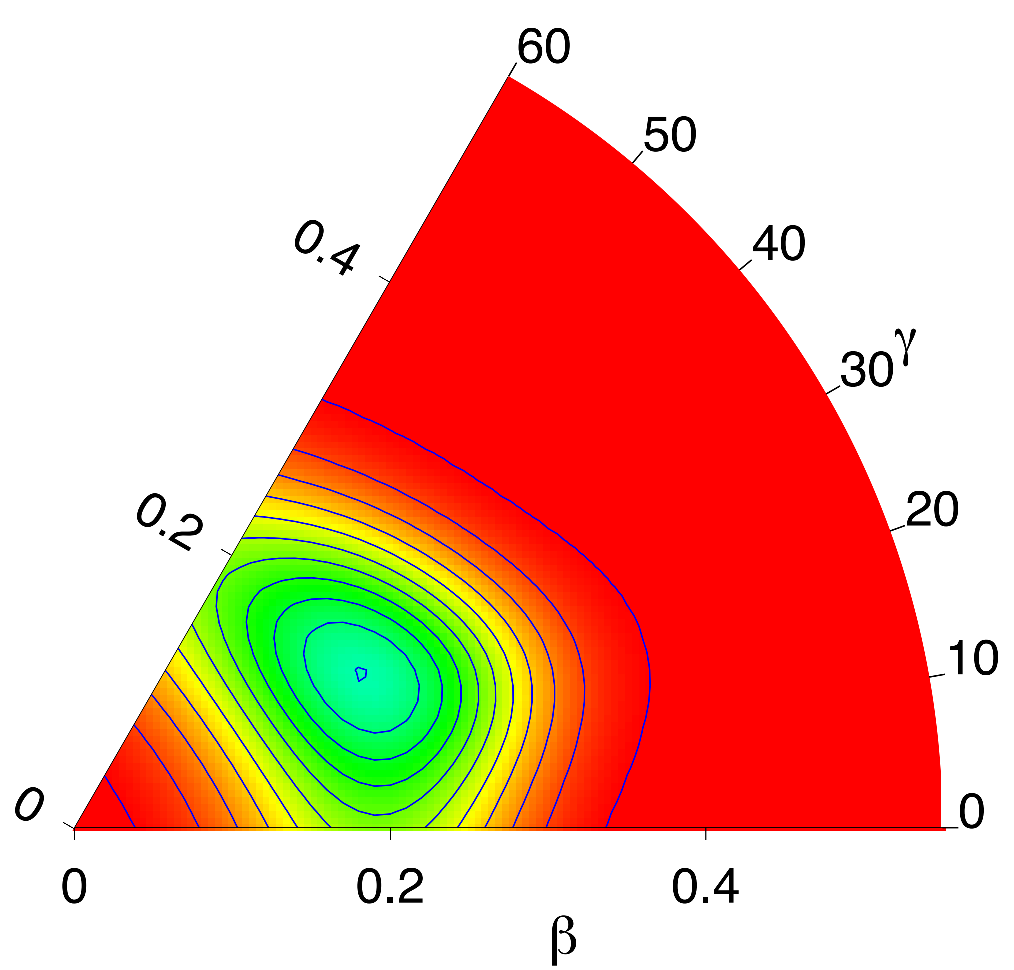

✓ TRIAXIAL calculations

✓ One single minimum in γ=30° and saddle points in the axial configurations

✓ PES very soft in the γ degree of freedom

✓ After GCM, there is not coexistence of prolate and oblate configurations for the ground state, just a triaxial state.

CONTENTS

The need of triaxiality: ^{126}Xe as an example

Triaxial calculations ^{126}Xe

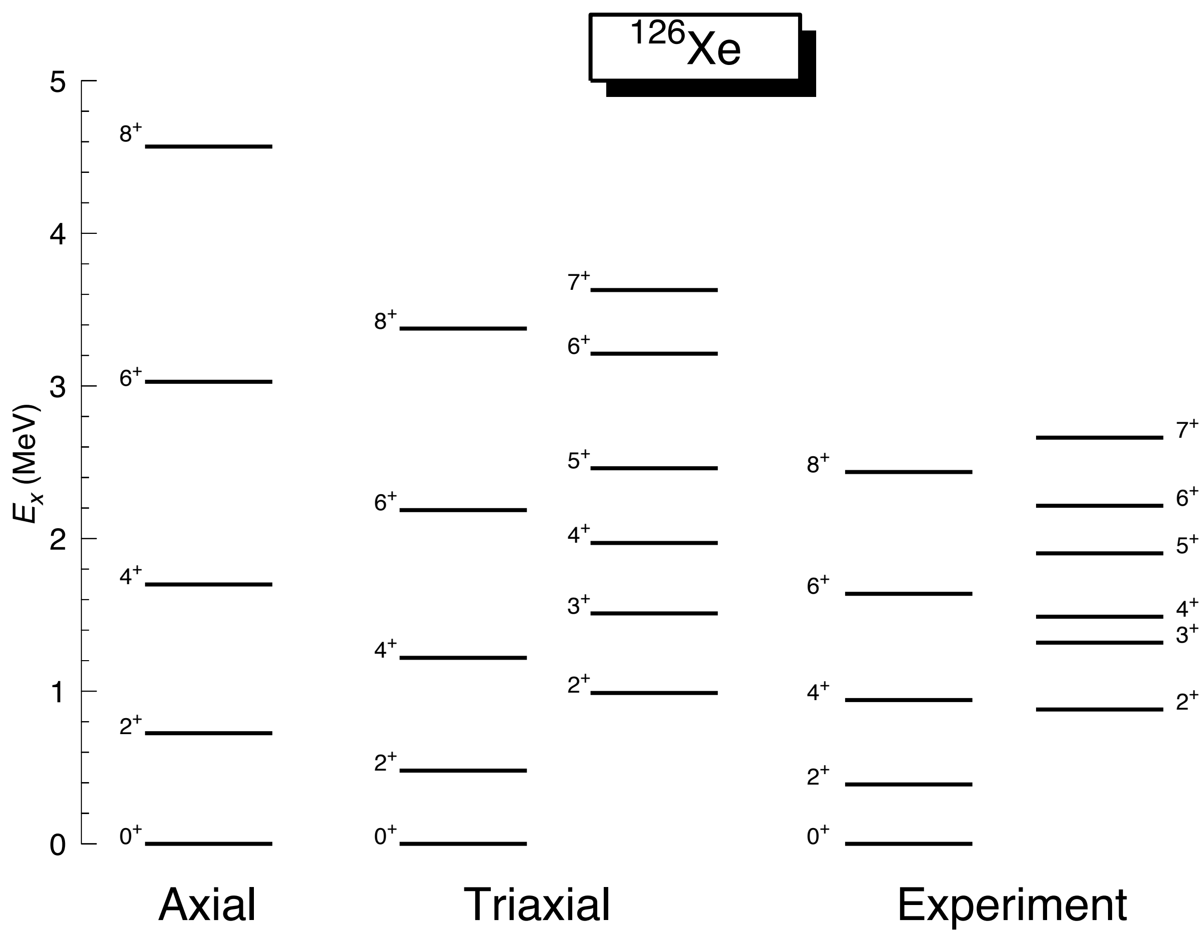

✓ TRIAXIAL calculations

✓ Triaxial calculations are able to describe qualitatively the experimental data

✓ Branching ratios for the B(E2) nicely reproduced.

$I_i \to I_f$	Exp.	Theory
$2_2^+ \to 2_1^+$	100.	100.
$2_2^+ \to 0_1^+$	1.5 $\pm$0.4	0.001
$3_1^+ \to 4_1^+$	$35.^{+10}_{-34}$	40.48
$3_1^+ \to 2_2^+$	100.	100.
$3_1^+ \to 2_1^+$	$2.0^{+0.6}_{-1.7}$	0.000
$4_2^+ \to 4_1^+$	76. $\pm$22	80.6
$4_2^+ \to 2_2^+$	100.	100.
$4_2^+ \to 2_1^+$	0.4$\pm$0.1	0.007
$5_1^+ \to 6_1^+$	75. $\pm$23	59.6
$5_1^+ \to 4_2^+$	76. $\pm$21	90.6
$5_1^+ \to 3_1^+$	100.	100.
$5_1^+ \to 4_1^+$	2.9 $\pm$0.8	0.02
$6_2^+ \to 6_1^+$	$34.\ ^{+15}_{-23}$	27.1
$6_2^+ \to 4_2^+$	100.	100.
$6_2^+ \to 4_1^+$	0.49 $\pm$0.15	0.003
$7_1^+ \to 6_2^+$	40. $\pm$26	45.11
$7_1^+ \to 5_1^+$	100.	100.

CONTENTS

The need of triaxiality: ^{126}Xe as an example

Triaxial calculations ^{126}Xe

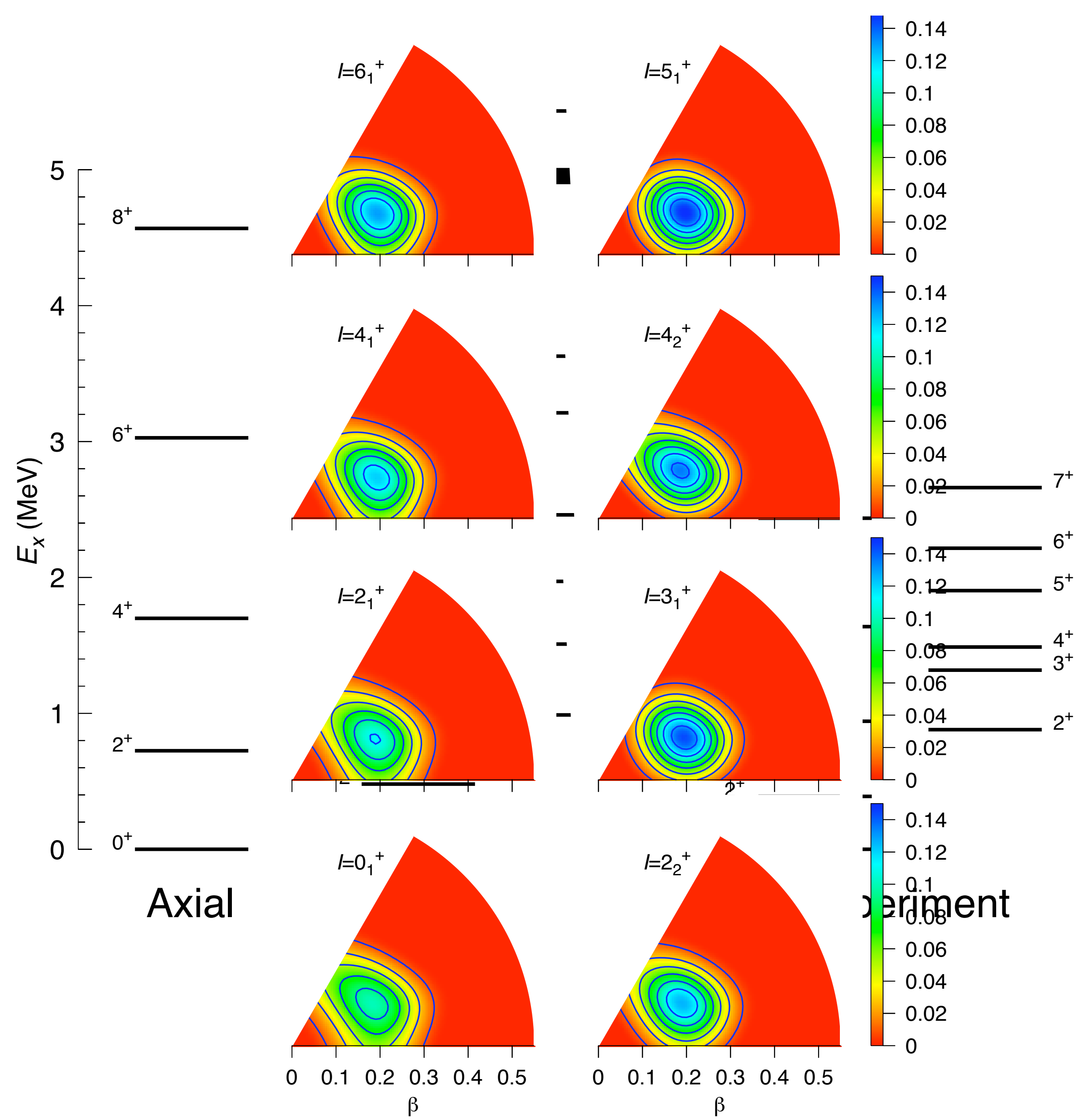

✓ TRIAXIAL calculations

✓ Triaxial calculations are able to describe qualitatively the experimental data

✓ Branching ratios for the B(E2) nicely reproduced.

$I_i \to I_f$	Exp.	Theory
$2_2^+ \to 2_1^+$	100.	100.
$2_2^+ \to 0_1^+$	1.5 ±0.4	0.001
$3_1^+ \to 4_1^+$	$35.^{+10}_{-34}$	40.48
$3_1^+ \to 2_2^+$	100.	100.
$3_1^+ \to 2_1^+$	$2.0^{+0.6}_{-1.7}$	0.000
$4_2^+ \to 4_1^+$	76. ±22	80.6
$4_2^+ \to 2_2^+$	100.	100.
$4_2^+ \to 2_1^+$	0.4±0.1	0.007
$5_1^+ \to 6_1^+$	75. ±23	59.6
$5_1^+ \to 4_2^+$	76. ±21	90.6
$5_1^+ \to 3_1^+$	100.	100.
$5_1^+ \to 4_1^+$	2.9 ±0.8	0.02
$6_2^+ \to 6_1^+$	$34.^{+15}_{-23}$	27.1
$6_2^+ \to 4_2^+$	100.	100.
$6_2^+ \to 4_1^+$	0.49 ±0.15	0.003
$7_1^+ \to 6_2^+$	40. ±26	45.11
$7_1^+ \to 5_1^+$	100.	100.

CONTENTS

The need of triaxiality: ^{126}Xe as an example

Triaxial calculations ^{126}Xe

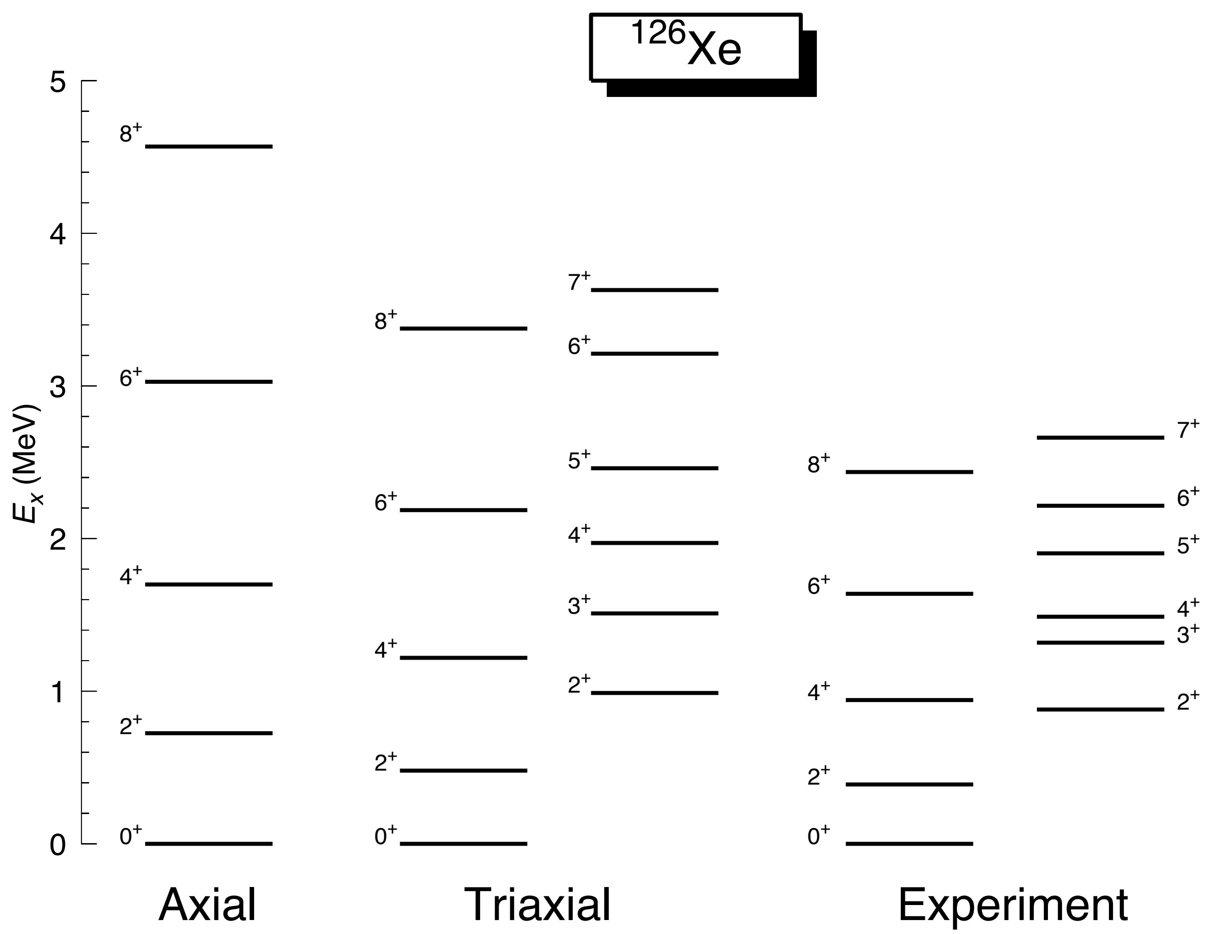

✓ TRIAXIAL calculations

✓ Triaxial calculations are able to describe qualitatively the experimental data

✓ Branching ratios for the B(E2) nicely reproduced.

$I_i \rightarrow I_f$	Exp.	Theory
$2_2^+ \rightarrow 2_1^+$	100.	100.
$2_2^+ \rightarrow 0_1^+$	1.5 $\pm$0.4	0.001
$3_1^+ \rightarrow 4_1^+$	35.$^{+10}_{-34}$	40.48
$3_1^+ \rightarrow 2_2^+$	100.	100.
$3_1^+ \rightarrow 2_1^+$	2.0$^{+0.6}_{-1.7}$	0.000
$4_2^+ \rightarrow 4_1^+$	76. $\pm$22	80.6
$4_2^+ \rightarrow 2_2^+$	100.	100.
$4_2^+ \rightarrow 2_1^+$	0.4$\pm$0.1	0.007
$5_1^+ \rightarrow 6_1^+$	75. $\pm$23	59.6
$5_1^+ \rightarrow 4_2^+$	76. $\pm$21	90.6
$5_1^+ \rightarrow 3_1^+$	100.	100.
$5_1^+ \rightarrow 4_1^+$	2.9 $\pm$0.8	0.02
$6_2^+ \rightarrow 6_1^+$	34. $^{+15}_{-23}$	27.1
$6_2^+ \rightarrow 4_2^+$	100.	100.
$6_2^+ \rightarrow 4_1^+$	0.49 $\pm$0.15	0.003
$7_1^+ \rightarrow 6_2^+$	40. $\pm$26	45.11
$7_1^+ \rightarrow 5_1^+$	100.	100.

Triaxial calculations ^{80}Zr

Motivation

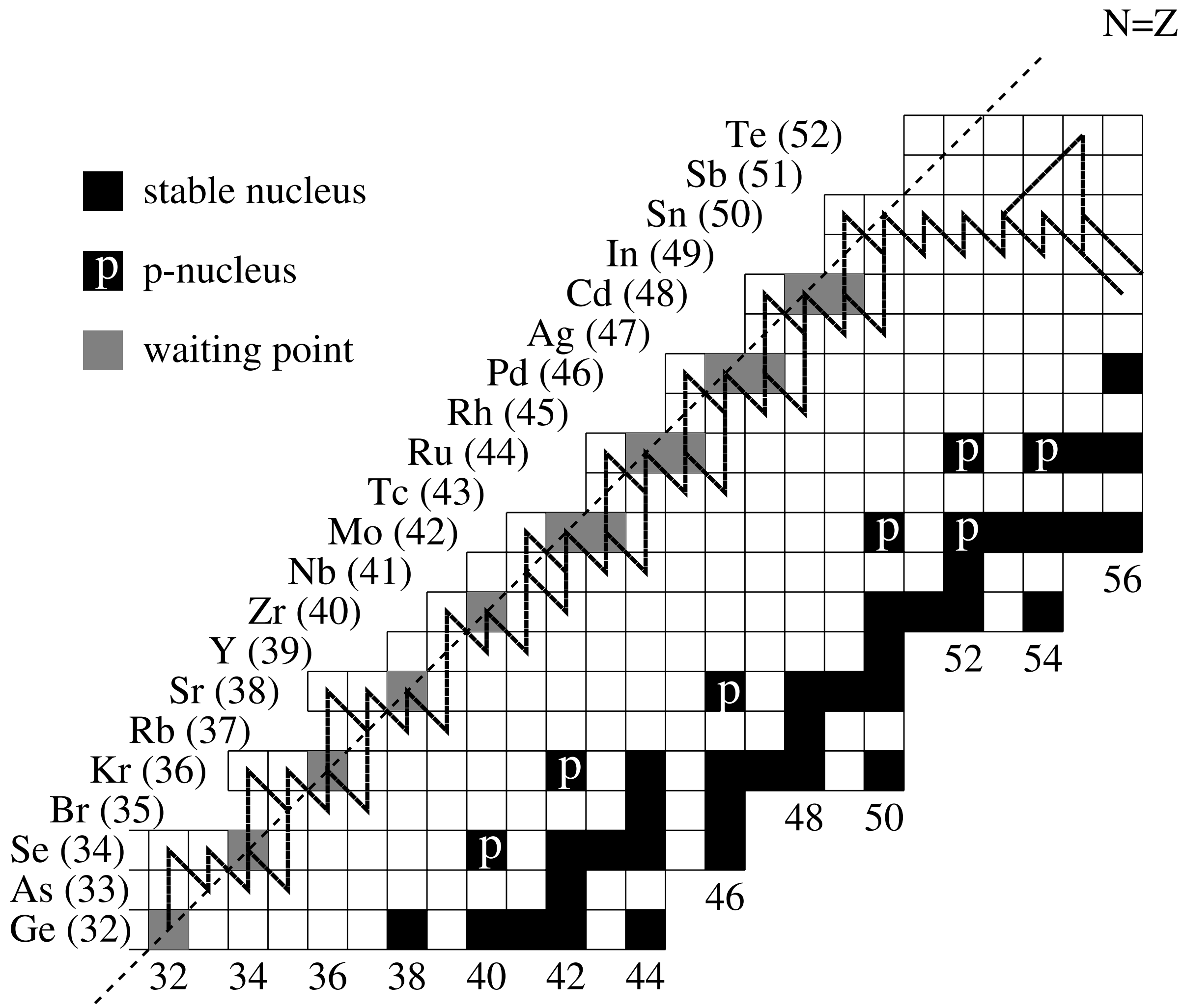

H. Schatz *et al.*, Phys. Rep. 294, 167 (1998)

✓ *N=Z* neutron deficient nuclei are the waiting points for rp-process nucleosynthesis

✓ Small proton capture cross sections and large beta half-lives

✓ Nuclear structure of these nuclei determines the parameters relevant to this process (masses, beta decay half-lives and branching ratios, ...)

Triaxial calculations ^{80}Zr

Motivation

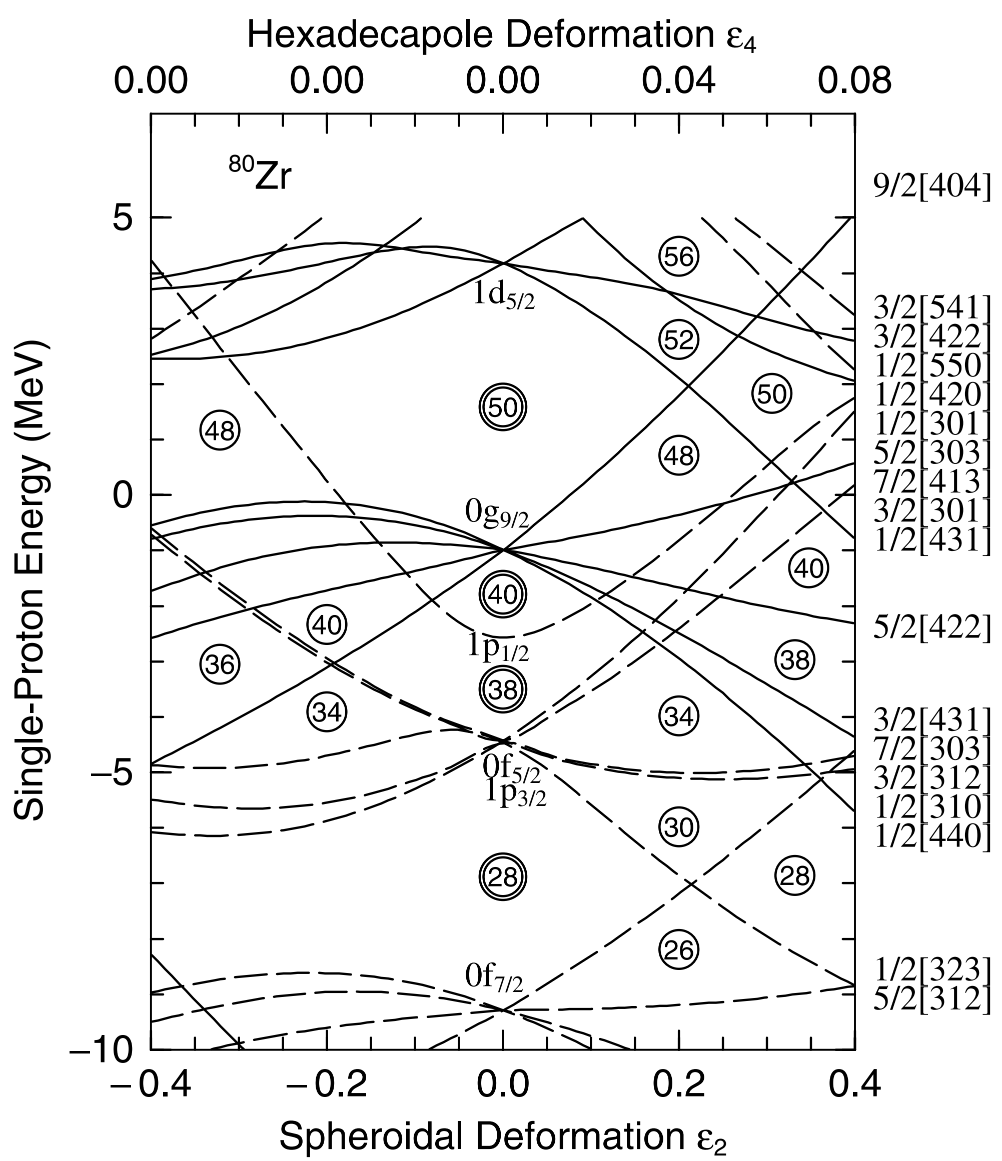

P. Möller *et al.*, At. Data Nucl. Data Tables 66,131 (1997)

✓ *N=Z* neutron deficient nuclei are the waiting points for rp-process nucleosynthesis

✓ Small proton capture cross sections and large beta half-lives

✓ Nuclear structure of these nuclei determines parameters relevant to this process (masses, beta decay half-lives and branching ratios, ...)

✓ Shape coexistence appears in most of these nuclei

✓ To which extent the appearance of "shape-isomeric" states affects the decay of these nuclei?

CONTENTS

Triaxial calculations ^{80}Zr

Motivation

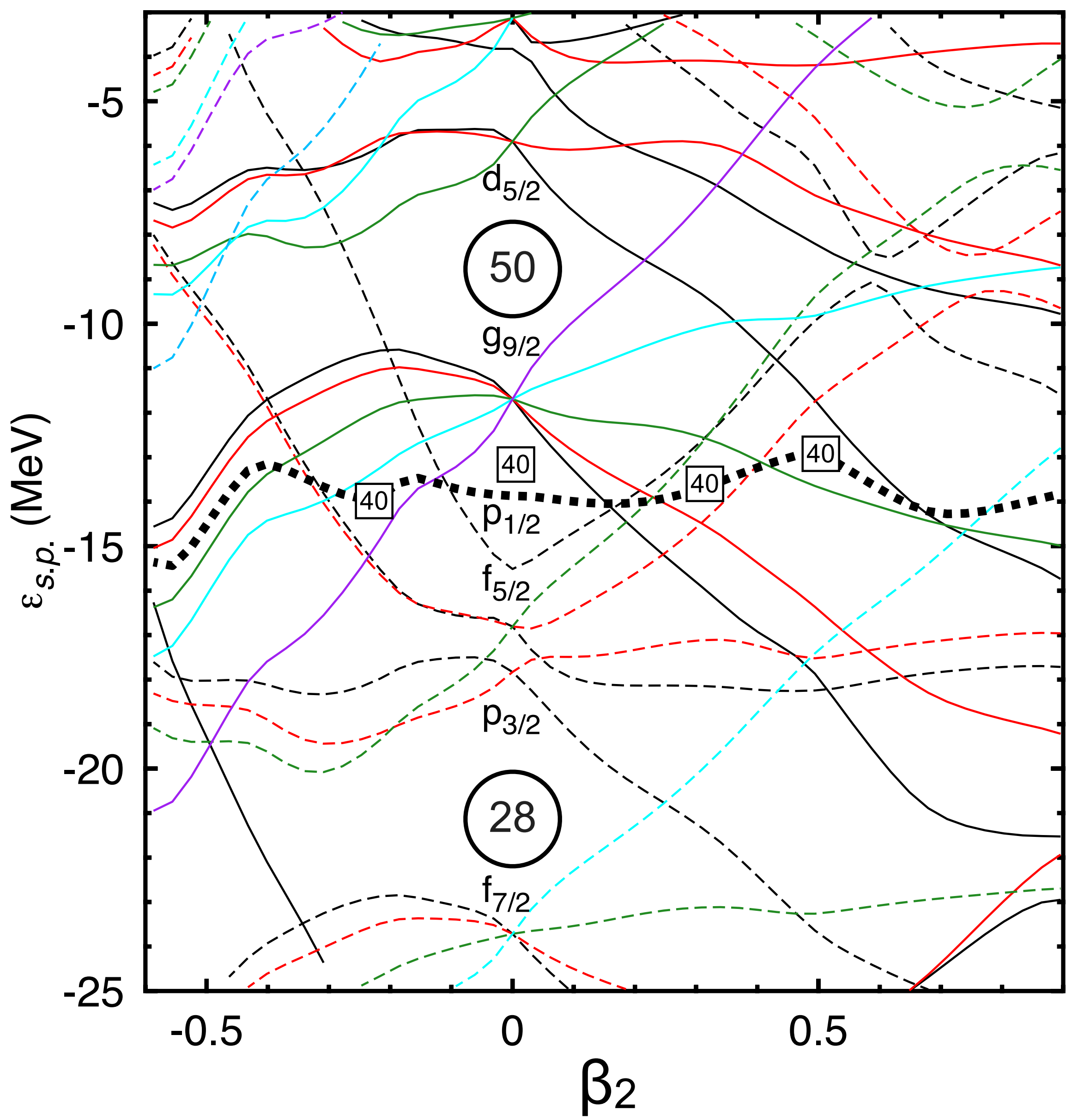

T.R.R. and J.L. Egido, submitted to PLB

✓ *N=Z* neutron deficient nuclei are the waiting points for rp-process nucleosynthesis

✓ Small proton capture cross sections and large beta half-lives

✓ Nuclear structure of these nuclei determines parameters relevant to this process (masses, beta decay half-lives and branching ratios, ...)

✓ Shape coexistence appears in most of these nuclei

✓ To which extent the appearance of “shape-isomeric” states affects the decay of these nuclei?

Triaxial calculations ^{80}Zr

Motivation

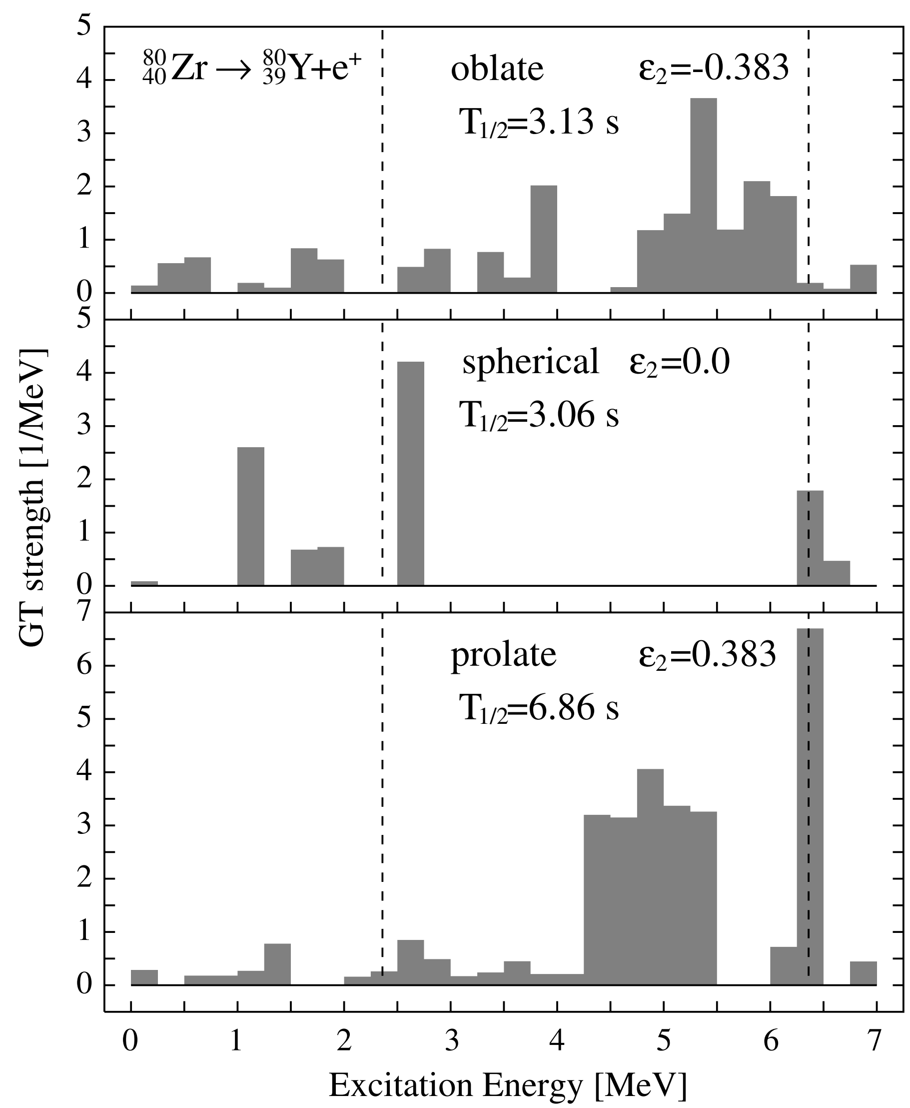

P. Möller *et al.*, At. Data Nucl. Data Tables 66,131 (1997)

✓ *N=Z* neutron deficient nuclei are the waiting points for rp-process nucleosynthesis

✓ Small proton capture cross sections and large beta half-lives

✓ Nuclear structure of these nuclei determines parameters relevant to this process (masses, beta decay half-lives and branching ratios, ...)

✓ Shape coexistence appears in most of these nuclei

✓ Different GT strength distribution depending on the shape of the mother nucleus.

Triaxial calculations ^{80}Zr

Motivation

CONTENTS

There are very few experimental data information of this nucleus:

- Ground state band energies (almost rotational)
(C.J. Lister et al, Phys. Rev. Lett. 59, 1270 (1987) and S. M. Fischer et al., Phys. Rev. Lett. 87, 132501 (2001))
- β^+ half-life (4.1 s)
(J. J. Ressler et al., Phys. Rev. Lett. 84, 2104 (2000))

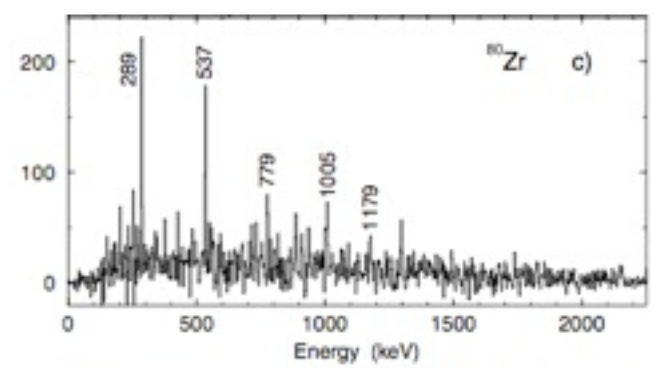

FIG. 1. Gamma-ray spectra of the ground state cascades in $N = Z$ nuclei: (a) ^{72}Kr (2α-gated $\gamma\gamma\gamma$ data, sum of $\gamma\gamma$ gates with one transition below and one transition above $J = 14$, production cross section $\sim 120\ \mu$b); (b) ^{76}Sr ($A/Q = 76/24$ and dE/dx gated $\gamma\gamma$ data, sum of γ gates for transitions below $J = 10$, $\sim 20\ \mu$b); (c) ^{80}Zr ($A/Q = 80/25$ and dE/dx gated γ singles, $\sim 10\ \mu$b).

S. M. Fischer et al., Phys. Rev. Lett. 87, 132501 (2001)

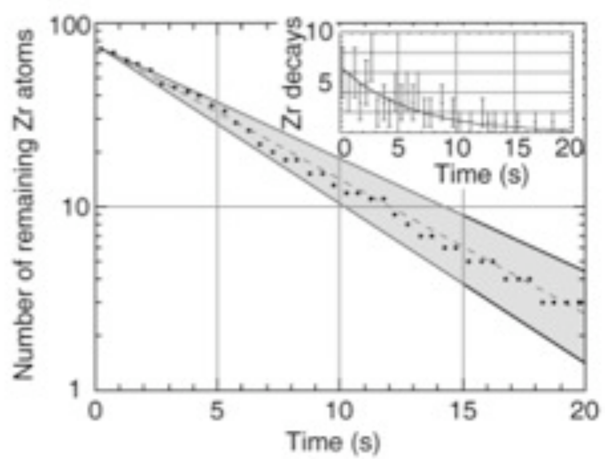

FIG. 4. Number of remaining Zr atoms as a function of time. The straight line represents a 4.1-s decay line, while the shaded areas show the range of error — 4.9 s as an upper limit and 3.5 s as a lower. The inset shows the background-corrected counts per 0.5 s.

J. J. Ressler et al., Phys. Rev. Lett. 84, 2104 (2000)

GSI theory HIC for FAIR

CONTENTS

Triaxial calculations ^{80}Zr

Motivation

There are very few experimental data information of this nucleus:

- Ground state band energies (almost rotational)

(C.J. Lister et al, Phys. Rev. Lett. 59, 1270 (1987) and S. M. Fischer et al., Phys. Rev. Lett. 87, 132501 (2001))

- β^+ half-life (4.1 s)

(J. J. Ressler et al., Phys. Rev. Lett. 84, 2104 (2000))

^{80}Zr:

✓ RELEVANT IN NUCLEOSYNTHESIS

✓ RELEVANT IN NUCLEAR STRUCTURE

FIG. 1. Gamma-ray spectra of the ground state cascades in $N = Z$ nuclei: (a) ^{72}Kr (2α-gated $\gamma\gamma\gamma$ data, sum of $\gamma\gamma$ gates with one transition below and one transition above $J = 14$, production cross section ~120 μb); (b) ^{76}Sr ($A/Q = 76/24$ and dE/dx gated $\gamma\gamma$ data, sum of γ gates for transitions below $J = 10$, ~20 μb); (c) ^{80}Zr ($A/Q = 80/25$ and dE/dx gated γ singles, ~10 μb).

S. M. Fischer et al., Phys. Rev. Lett. 87, 132501 (2001)

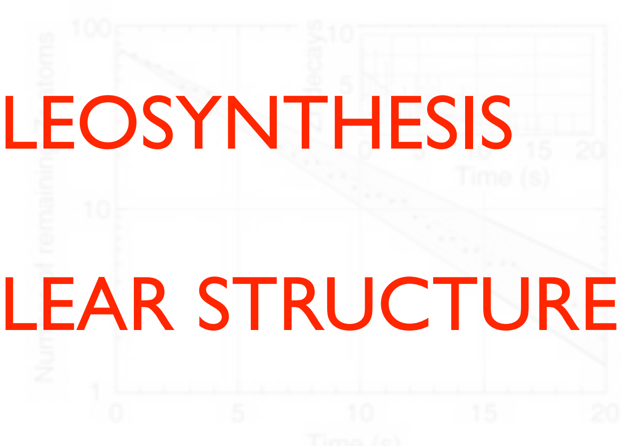

FIG. 4. Number of remaining Zr atoms as a function of time. The straight line represents a 4.1-s decay line, while the shaded areas show the range of error — 4.9 s as an upper limit and 3.5 s as a lower. The inset shows the background-corrected counts per 0.5 s.

J. J. Ressler et al., Phys. Rev. Lett. 84, 2104 (2000)

Triaxial calculations ^{80}Zr

First step: Particle Number Projection (before the variation) of HFB-type wave functions.

$$\delta E^{N,Z}\left[\bar{\Phi}(\beta,\gamma)\right]\Big|_{\bar{\Phi}=\Phi}=0 \quad E^{N,Z}[\Phi]=\frac{\langle\Phi|\hat{H}_{2\mathrm{b}}\hat{P}^{N}\hat{P}^{Z}|\Phi\rangle}{\langle\Phi|\hat{P}^{N}\hat{P}^{Z}|\Phi\rangle}+\varepsilon_{DD}^{N,Z}(\Phi)-\lambda_{q_{20}}\langle\Phi|\hat{Q}_{20}|\Phi\rangle-\lambda_{q_{22}}\langle\Phi|\hat{Q}_{22}|\Phi\rangle$$

CONTENTS

CONTENTS

Triaxial calculations ^{80}Zr

First step: Particle Number Projection (before the variation) of HFB-type wave functions.

$$\delta E^{N,Z}\left[\bar{\Phi}(\beta,\gamma)\right]\Big|_{\bar{\Phi}=\Phi}=0 \quad E^{N,Z}[\Phi]=\frac{\langle\Phi|\hat{H}_{2b}\hat{P}^N\hat{P}^Z|\Phi\rangle}{\langle\Phi|\hat{P}^N\hat{P}^Z|\Phi\rangle}+\varepsilon_{DD}^{N,Z}(\Phi)-\lambda_{q_{20}}\langle\Phi|\hat{Q}_{20}|\Phi\rangle-\lambda_{q_{22}}\langle\Phi|\hat{Q}_{22}|\Phi\rangle$$

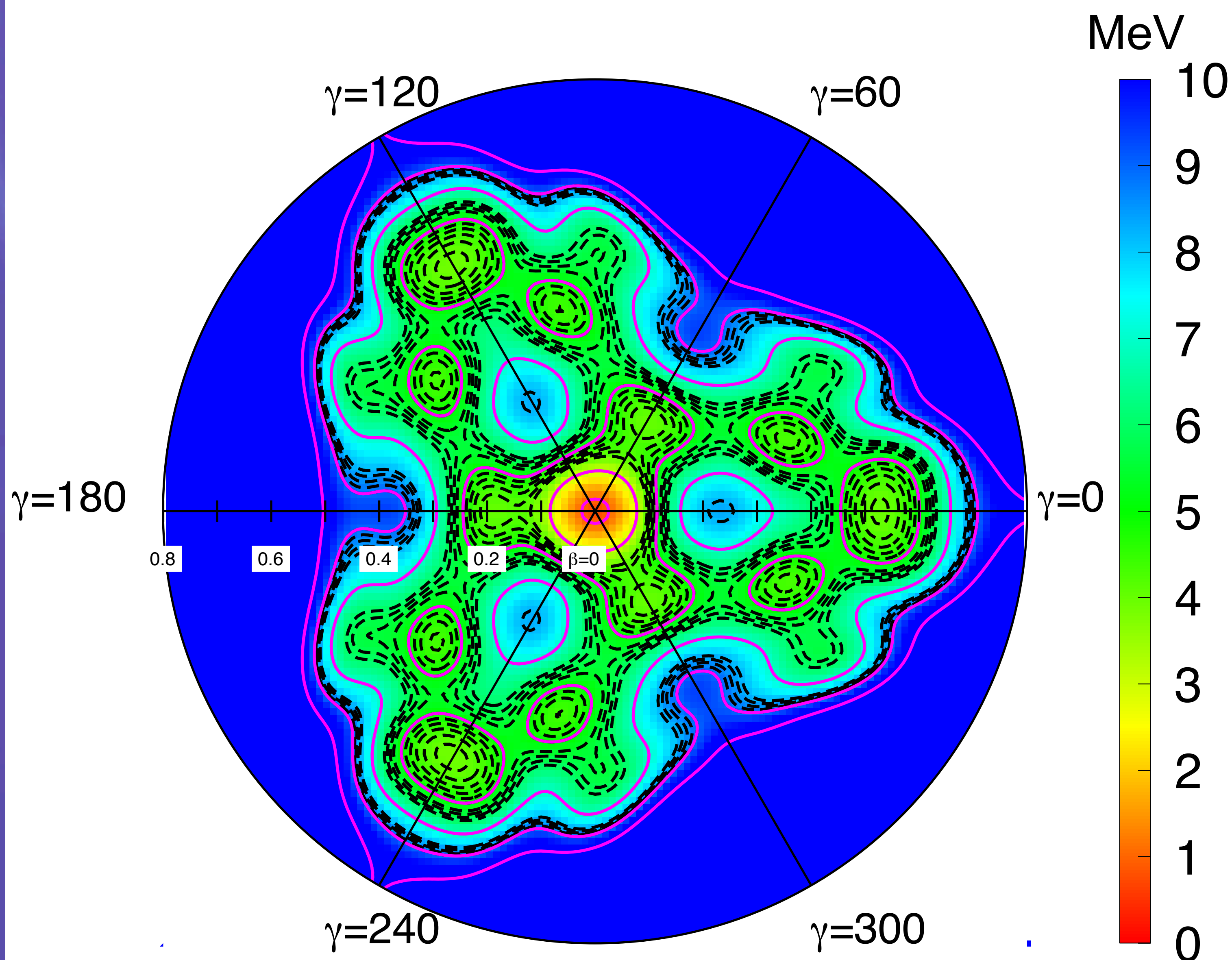

- Symmetry corresponding to the different orientation of the axes
- All configurations are included between γ∈[0º,60º]

CONTENTS

Triaxial calculations ^{80}Zr

First step: Particle Number Projection (before the variation) of HFB-type wave functions.

$$\delta E^{N,Z}\left[\bar{\Phi}(\beta,\gamma)\right]\Big|_{\bar{\Phi}=\Phi}=0 \quad E^{N,Z}[\Phi]=\frac{\langle\Phi|\hat{H}_{2b}\hat{P}^{N}\hat{P}^{Z}|\Phi\rangle}{\langle\Phi|\hat{P}^{N}\hat{P}^{Z}|\Phi\rangle}+\varepsilon_{DD}^{N,Z}(\Phi)-\lambda_{q_{20}}\langle\Phi|\hat{Q}_{20}|\Phi\rangle-\lambda_{q_{22}}\langle\Phi|\hat{Q}_{22}|\Phi\rangle$$

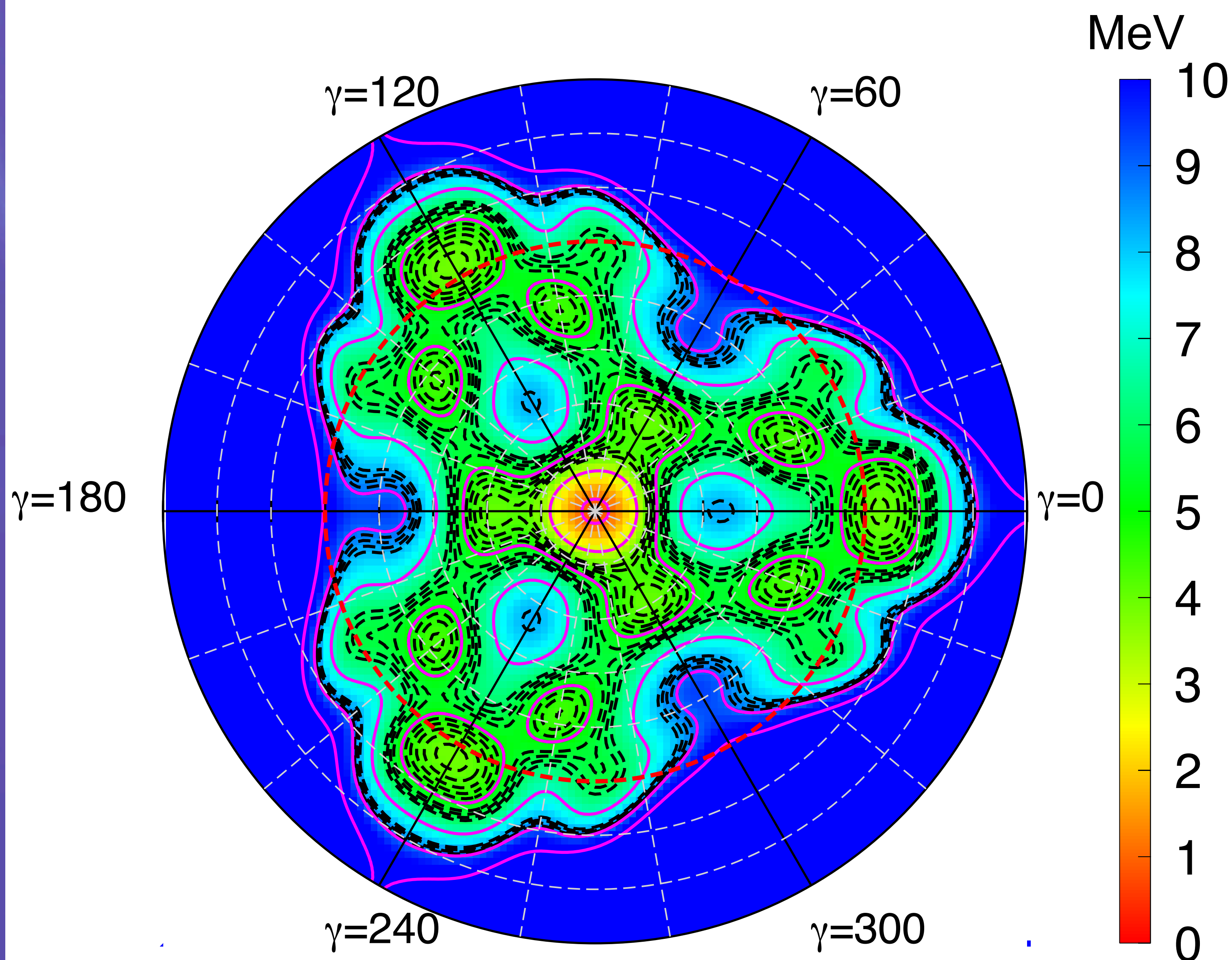

- Symmetry corresponding to the different orientation of the axes
- All configurations are included between γ∈[0º,60º]

CONTENTS

Triaxial calculations ^{80}Zr

First step: Particle Number Projection (before the variation) of HFB-type wave functions.

$$\delta E^{N,Z}\left[\bar{\Phi}(\beta,\gamma)\right]\Big|_{\bar{\Phi}=\Phi}=0 \qquad E^{N,Z}[\Phi]=\frac{\langle\Phi|\hat{H}_{2b}\hat{P}^{N}\hat{P}^{Z}|\Phi\rangle}{\langle\Phi|\hat{P}^{N}\hat{P}^{Z}|\Phi\rangle}+\varepsilon_{DD}^{N,Z}(\Phi)-\lambda_{q_{20}}\langle\Phi|\hat{Q}_{20}|\Phi\rangle-\lambda_{q_{22}}\langle\Phi|\hat{Q}_{22}|\Phi\rangle$$

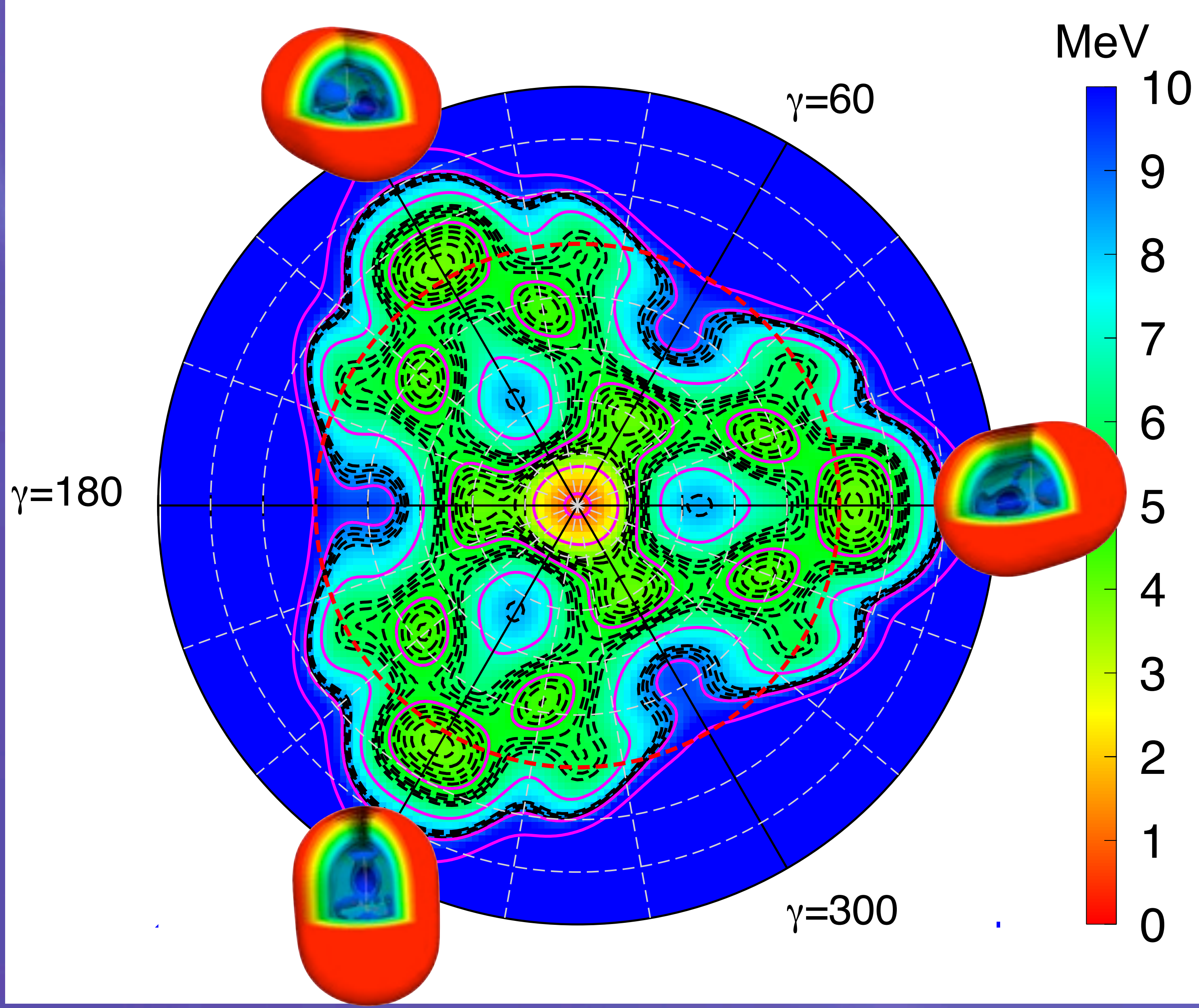

- Symmetry corresponding to the different orientation of the axes
- All configurations are included between γ∈[0º,60º]

Triaxial calculations ^{80}Zr

CONTENTS

First step: Particle Number Projection (before the variation) of HFB-type wave functions.

$$\delta E^{N,Z}\left[\bar{\Phi}(\beta,\gamma)\right]\Big|_{\bar{\Phi}=\Phi}=0 \quad E^{N,Z}[\Phi]=\frac{\langle\Phi|\hat{H}_{2b}\hat{P}^N\hat{P}^Z|\Phi\rangle}{\langle\Phi|\hat{P}^N\hat{P}^Z|\Phi\rangle}+\varepsilon_{DD}^{N,Z}(\Phi)-\lambda_{q_{20}}\langle\Phi|\hat{Q}_{20}|\Phi\rangle-\lambda_{q_{22}}\langle\Phi|\hat{Q}_{22}|\Phi\rangle$$

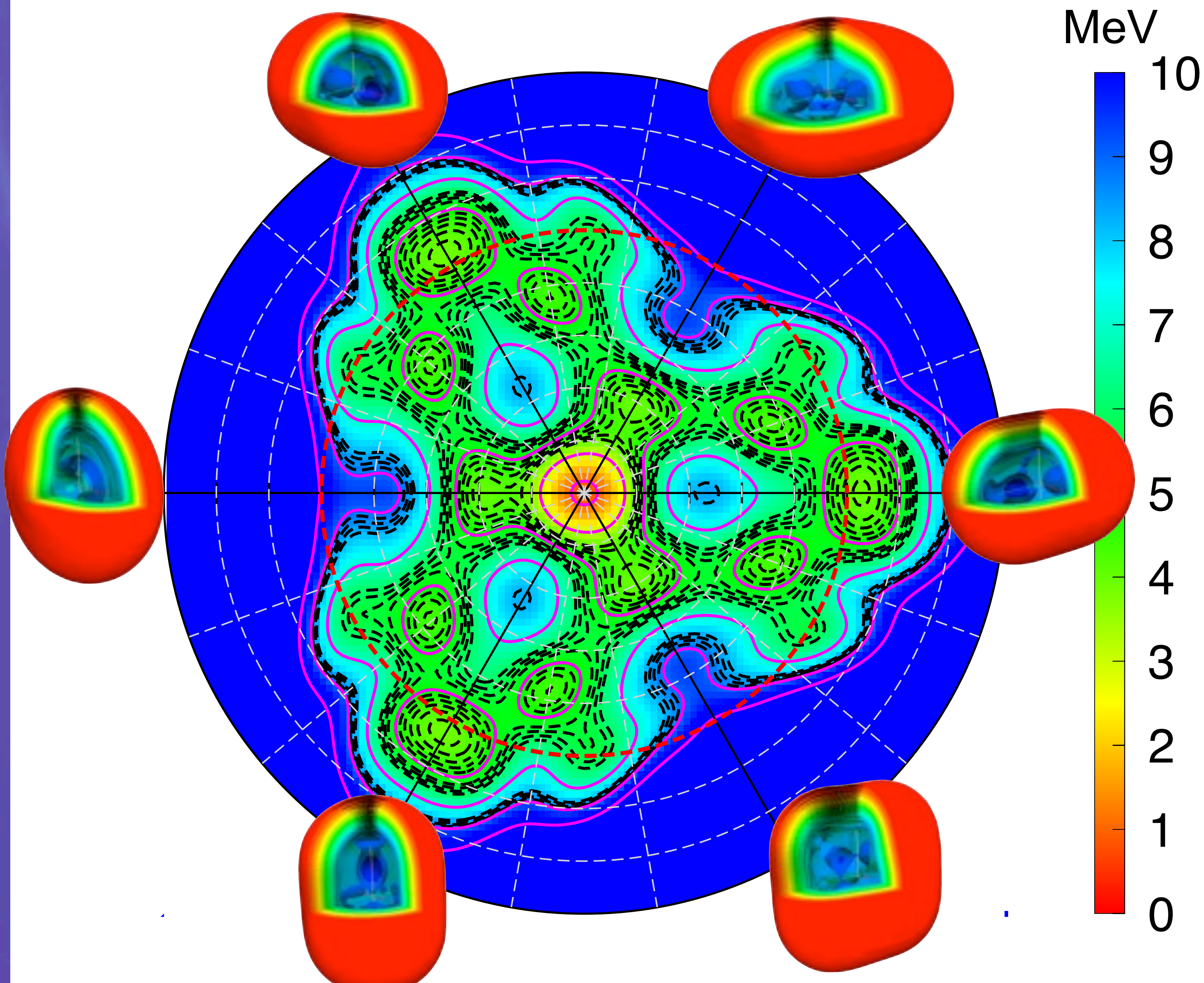

- Symmetry corresponding to the different orientation of the axes
- All configurations are included between γ∈[0º,60º]

Triaxial calculations ^{80}Zr

First step: Particle Number Projection (before the variation) of HFB-type wave functions.

$$\delta E^{N,Z}\left[\bar{\Phi}(\beta,\gamma)\right]\Big|_{\bar{\Phi}=\Phi}=0 \qquad E^{N,Z}[\Phi]=\frac{\langle\Phi|\hat{H}_{2b}\hat{P}^N\hat{P}^Z|\Phi\rangle}{\langle\Phi|\hat{P}^N\hat{P}^Z|\Phi\rangle}+\varepsilon_{DD}^{N,Z}(\Phi)-\lambda_{q_{20}}\langle\Phi|\hat{Q}_{20}|\Phi\rangle-\lambda_{q_{22}}\langle\Phi|\hat{Q}_{22}|\Phi\rangle$$

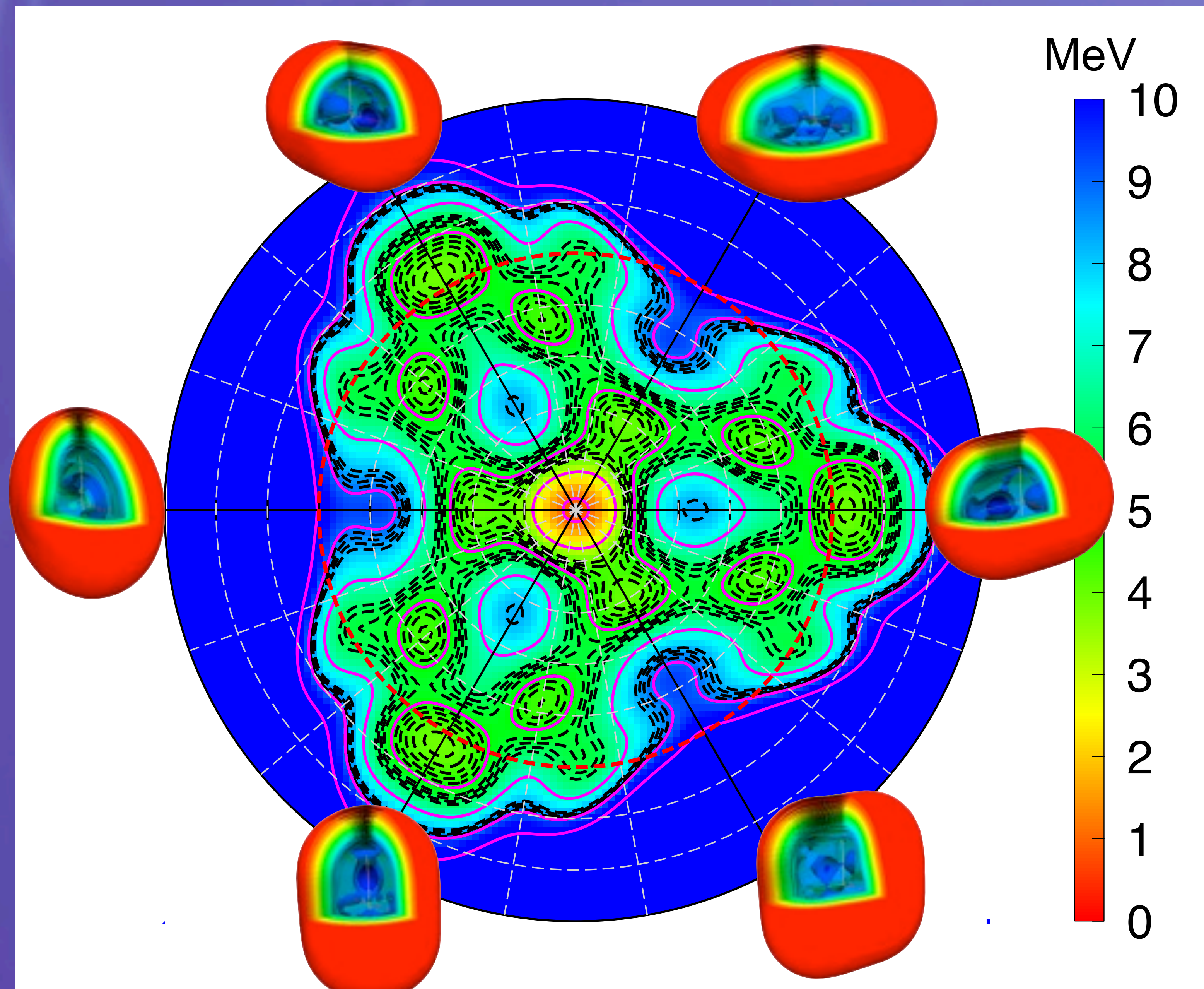

- Symmetry corresponding to the different orientation of the axes
- All configurations are included between γ∈[0º,60º]

GSI theory HIC for FAIR

CONTENTS

Triaxial calculations ^{80}Zr (83 states, 9 shells)

First step: Particle Number Projection (before the variation) of HFB-type wave functions.

$$\delta E^{N,Z}\left[\bar{\Phi}(\beta,\gamma)\right]\Big|_{\bar{\Phi}=\Phi}=0 \qquad E^{N,Z}[\Phi]=\frac{\langle\Phi|\hat{H}_{2b}\hat{P}^{N}\hat{P}^{Z}|\Phi\rangle}{\langle\Phi|\hat{P}^{N}\hat{P}^{Z}|\Phi\rangle}+\varepsilon^{N,Z}_{DD}(\Phi)-\lambda_{q_{20}}\langle\Phi|\hat{Q}_{20}|\Phi\rangle-\lambda_{q_{22}}\langle\Phi|\hat{Q}_{22}|\Phi\rangle$$

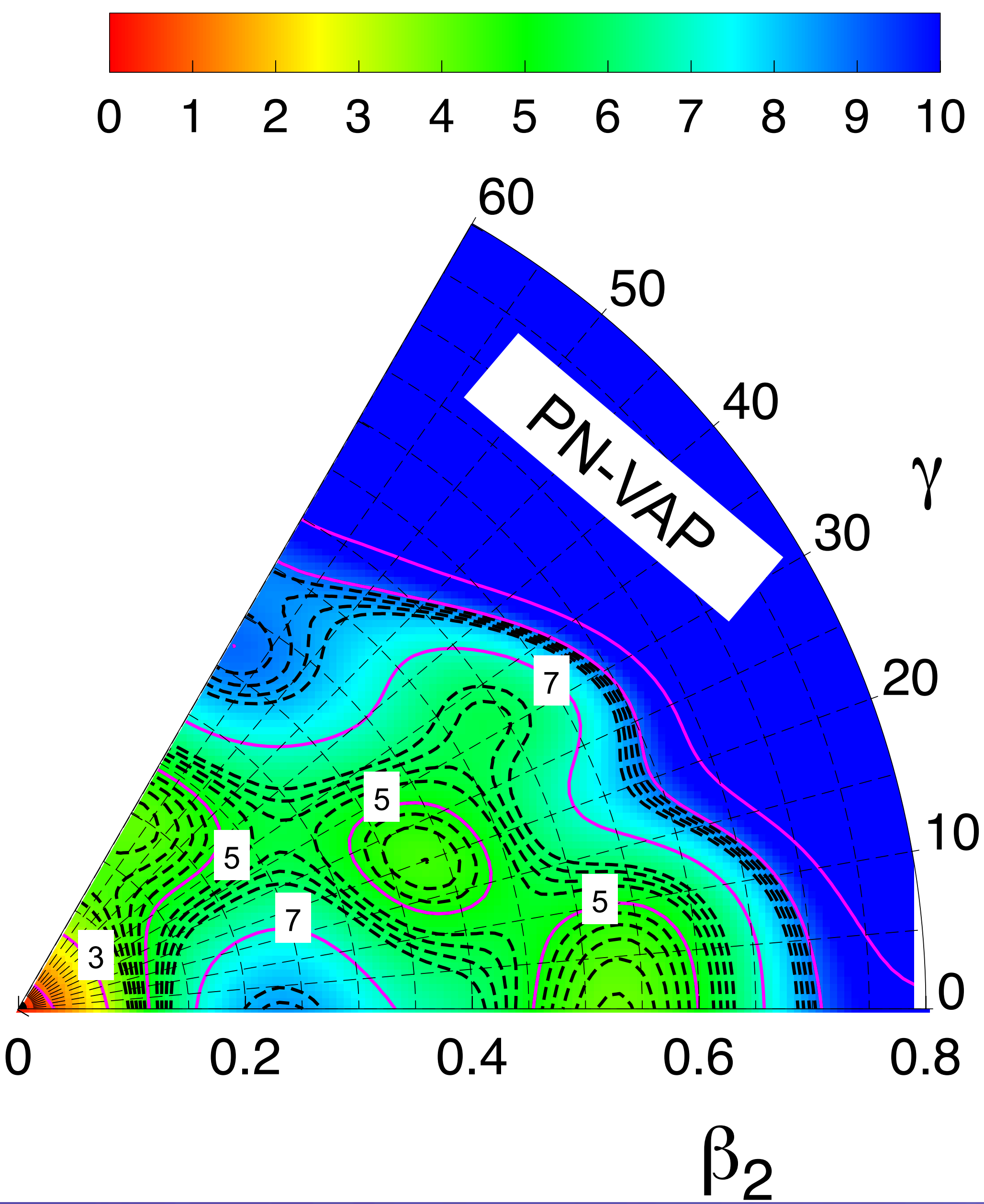

- Up to five minima in the potential energy surface.
- Absolute minimum corresponds to spherical configuration (N=40 spherical gap)
- Other minima related to the filling in and out of $g_{9/2}$, $p_{1/2}$, $f_{5/2}$ and $d_{5/2}$ orbits.

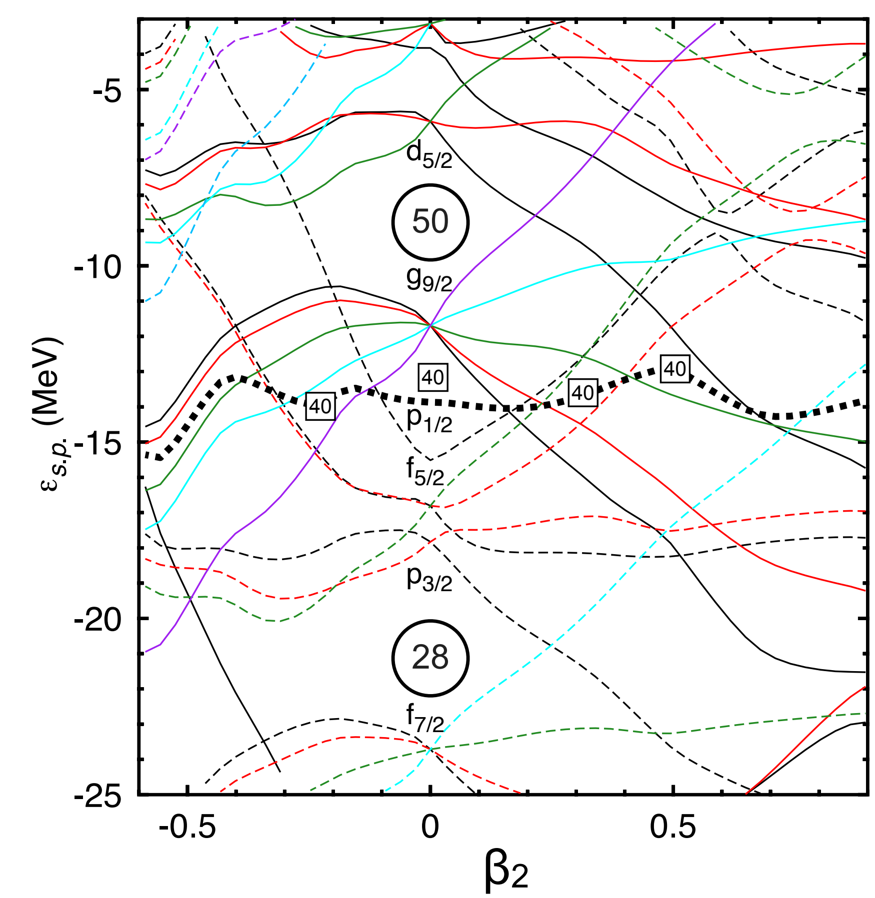

Triaxial calculations ^{80}Zr (83 states, 9 shells)

Second step: Simultaneous **Particle Number and Angular Momentum Projection**

$$|IMK;NZ;\beta\gamma\rangle = \frac{2I+1}{8\pi^2}\int \mathcal{D}^{I*}_{MK}(\Omega)\hat{R}(\Omega)\hat{P}^N\hat{P}^Z|\Phi(\beta,\gamma)\rangle d\Omega \rightarrow |IM;NZ;\beta\gamma\rangle = \sum_K g_K^{IM;NZ;\beta\gamma}|IMK;NZ;\beta\gamma\rangle$$

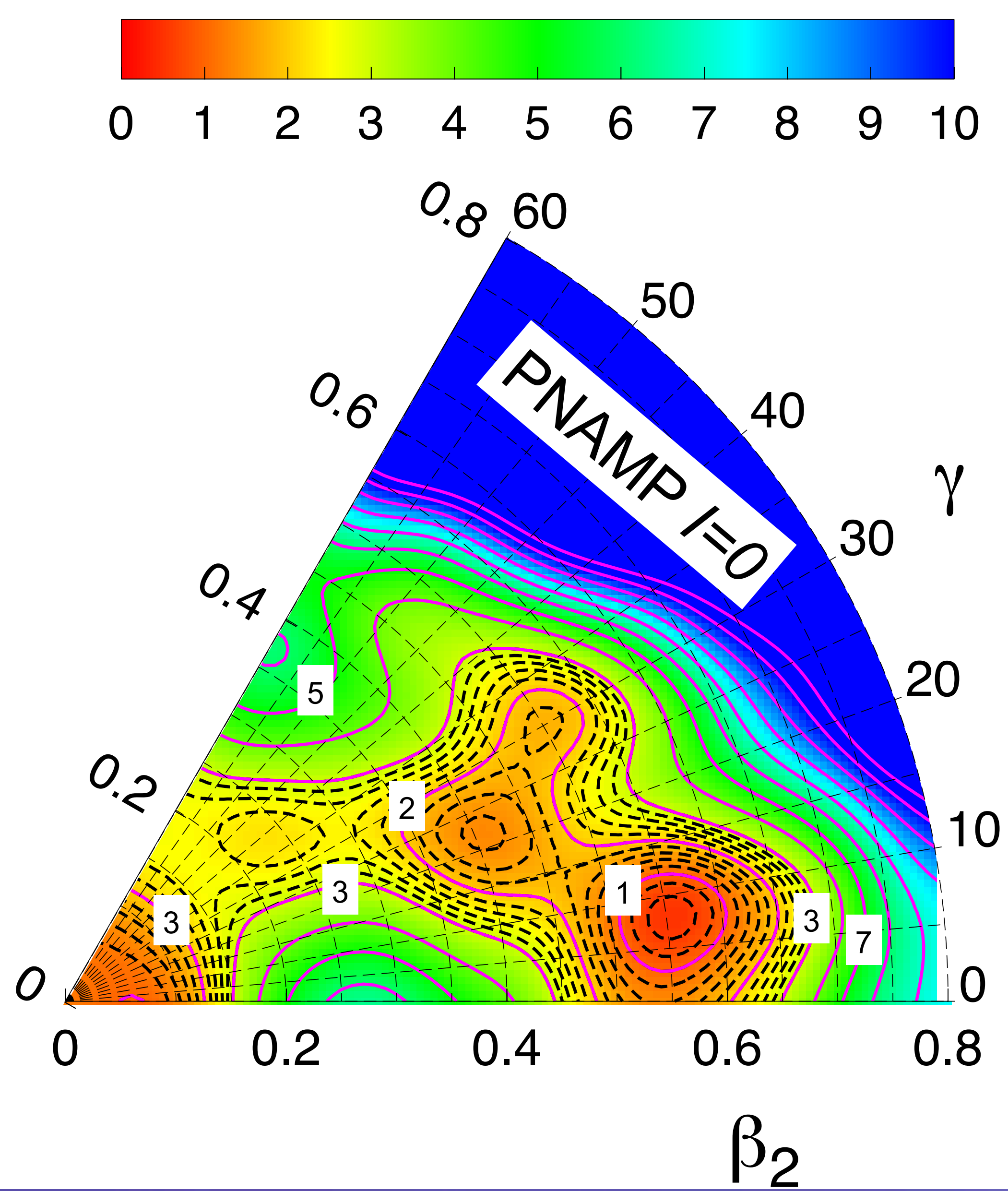

- Five minima are closer in energy whenever the rotational invariance is restored.
- Absolute minima corresponds to deformed configuration β~0.55
- Barriers between the minima are less than 1 MeV. Mixing?

Triaxial calculations ^{80}Zr (83 states, 9 shells)

Second step: Simultaneous **Particle Number and Angular Momentum Projection**

$$|IMK;NZ;\beta\gamma\rangle=\frac{2I+1}{8\pi^2}\int\mathcal{D}^{I*}_{MK}(\Omega)\hat{R}(\Omega)\hat{P}^N\hat{P}^Z|\Phi(\beta,\gamma)\rangle d\Omega\;\rightarrow\;|IM;NZ;\beta\gamma\rangle=\sum_K g_K^{IM;NZ;\beta\gamma}|IMK;NZ;\beta\gamma\rangle$$

CONTENTS

1. Theoretical framework

Relevance of angular momentum projection

(Similar feature as in ^{32}Mg, see R. Rodriguez-Guzmán et al., Nucl. Phys. A 709, 201 (2002))

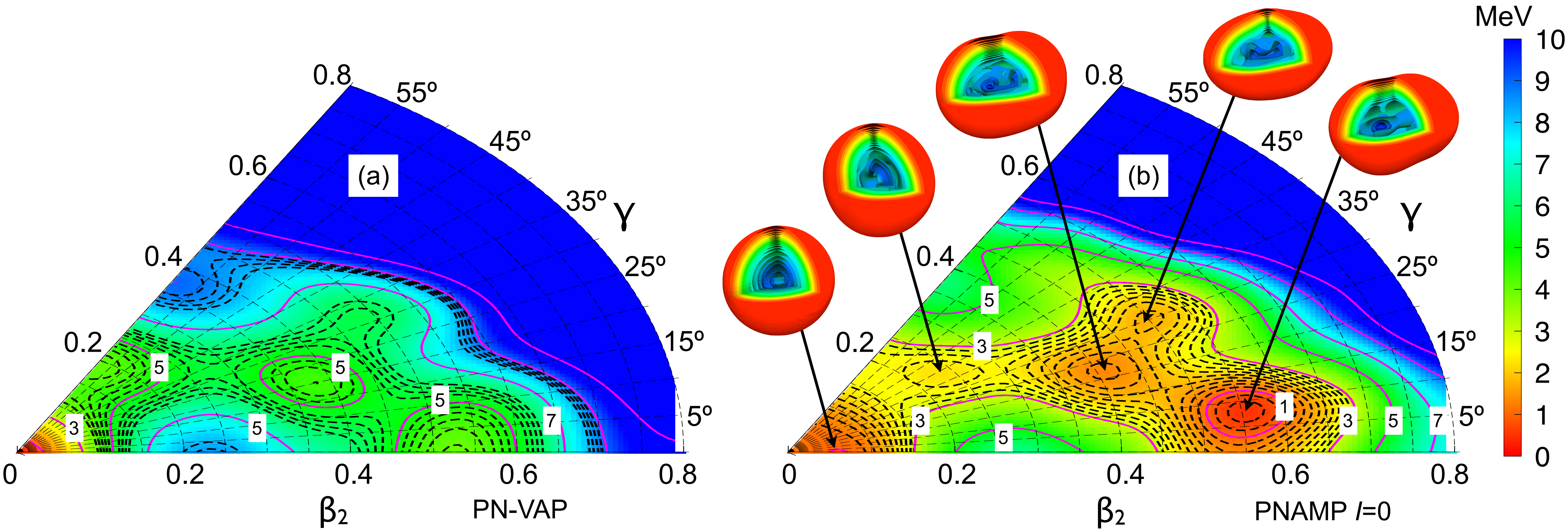

CONTENTS

Triaxial calculations ^{80}Zr (83 states, 9 shells)

Final step: Configuration mixing within the framework of the **Generator Coordinate Method (GCM)**. ***K* and deformation mixing**

$$|IM;NZ\sigma\rangle=\sum_{K\beta\gamma}f^{I;NZ,\sigma}_{K\beta\gamma}|IMK;NZ;\beta\gamma\rangle$$

T.R.R and J.L. Egido, Phys. Lett. B submitted.

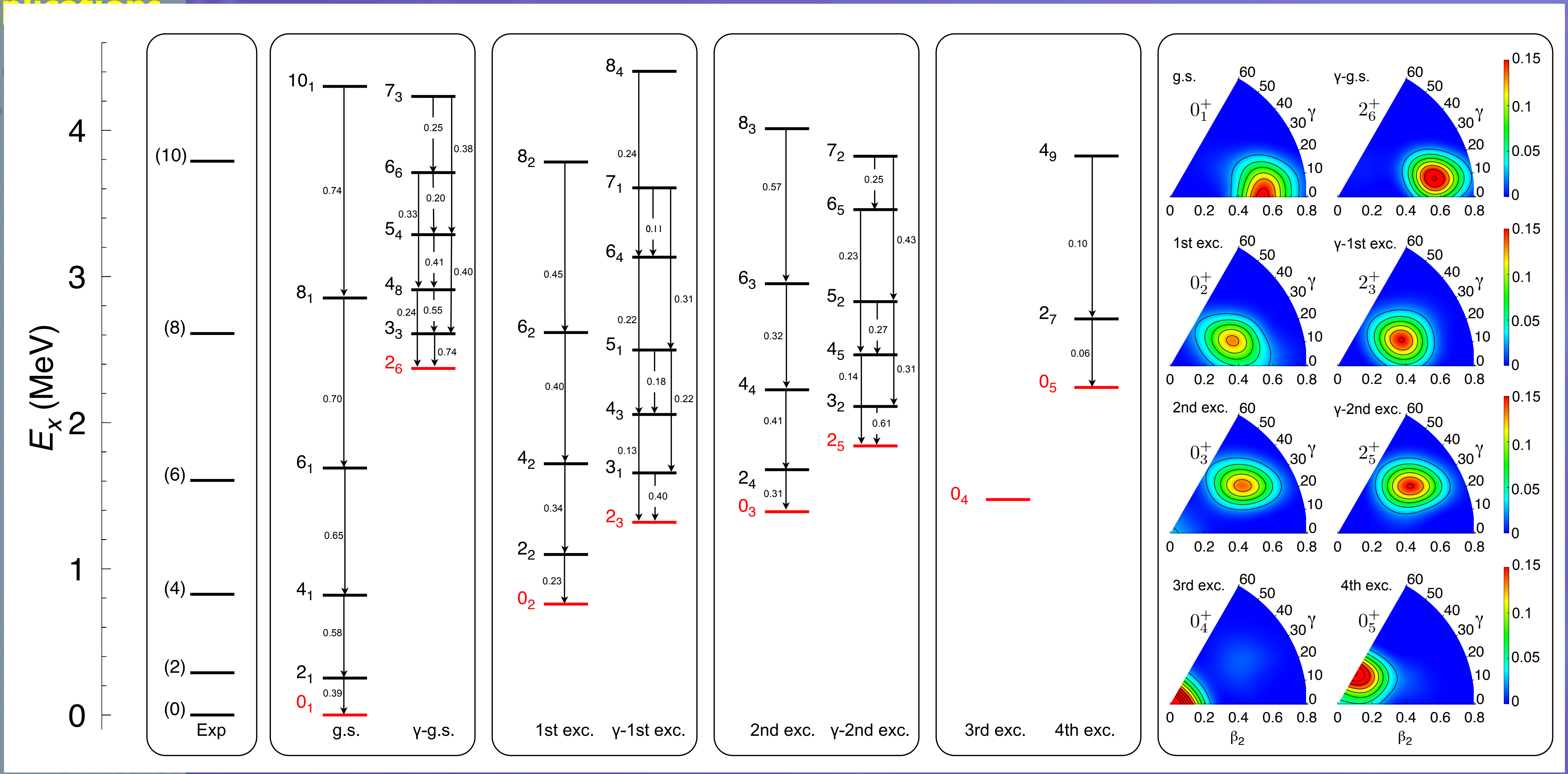

Triaxial calculations ^{80}Zr (83 states, 9 shells)

Final step: Configuration mixing within the framework of the **Generator Coordinate Method (GCM)**. ***K* and deformation mixing**

$$|IM;NZ\sigma\rangle = \sum_{K\beta\gamma} f^{I;NZ,\sigma}_{K\beta\gamma}|IMK;NZ;\beta\gamma\rangle$$

T.R.R and J.L. Egido, Phys. Lett. B submitted.

-Several rotational bands and gamma bands partners associated to the different minima of the potential energy surfaces.

- Axial ground state rotational band in agreement with the experimental levels (relevance of beyond-mean-field effects).

- Two triaxial rotational bands.

- Four excited 0^+ minima within a range of ~2.25 MeV ⇒ MULTISHAPE COEXISTENCE

- However, these levels are not thermally populated in astrophysical conditions (T~100 keV)

- Electromagnetic transitions are much faster than beta decay half-lives ⇒ NO INFLUENCE in the rp process nucleosynthesis

CONTENTS

Conclusions and outlook

✓ Current phenomenological Energy Density Functional methods including triaxial shapes provide a very good description and physical insight of many phenomena in nuclei along the whole nuclear chart.

✓ It is a competitive alternative and/or complement to shell model calculations.

✓ Computational time is still a problem.

✓ Some improvements have to be performed yet:

- Projection of cranking states (time reversal symmetry breaking).
- Include quasiparticle states (blocking) to describe single particle excitations, odd nuclei and β transitions.
- Include parity and isospin breaking.
- Fit the interaction with beyond mean field calculations (relevant to mass table calculations) and/or develop new non-empirical functionals based on QCD (relevant to mass table calculations).

Acknowledgments

J. L. Egido (Universidad Autónoma de Madrid)

G. Martínez-Pinedo (GSI-Darmstadt)
Andrea Jungclaus (IEMM-CSIC Madrid)
C. Domingo-Pardo (IFIC-CSIC Valencia)
Nuria López Vaquero (Universidad Autónoma de Madrid)

THANK YOU FOR YOUR ATTENTION!!!